SKB

TECHNICAL REPORT 94-31

The implications of soil acidification on a future HLW repository

Part II: Influence on deep granitic groundwater. The Klipperås study site as test case

Paul Wersin[1], Jordi Bruno[1], Marcus Laaksoharju[2]

1 MBT Technología Ambiental, Cerdanyola, Spain
2 Geopoint AB, Spånga, Sweden

May 1994

SVENSK KÄRNBRÄNSLEHANTERING AB
SWEDISH NUCLEAR FUEL AND WASTE MANAGEMENT CO

BOX 5864 S-102 40 STOCKHOLM
TEL. 08-665 28 00 TELEX 13108 SKB
TELEFAX 08-661 57 19

THE IMPLICATIONS OF SOIL ACIDIFICATION ON A FUTURE HLW REPOSITORY

PART II: INFLUENCE ON DEEP GRANITIC GROUNDWATER. THE KLIPPERÅS STUDY SITE AS TEST CASE

Paul Wersin[1], Jordi Bruno[1], Marcus Laaksoharju[2]

1 **MBT Tecnología Ambiental, Cerdanyola, Spain**
2 **Geopoint AB, Spånga, Sweden**

May 1994

THE IMPLICATIONS OF SOIL ACIDIFICATION ON A FUTURE HLW REPOSITORY.

PART II: INFLUENCE ON DEEP GRANITIC GROUNDWATER. THE KLIPPERÅS STUDY SITE AS TEST CASE

Paul Wersin[1], Jordi Bruno[1], Marcus Laaksoharju[2]

[1]MBT Tecnología Ambiental, Cerdanyola, Spain
[2]Geopoint AB, Spånga, Sweden

May 1994

Abstract

The effect of acidification on deep groundwater is assessed with a geochemical box model based on the STEADYQL code. The application of the model to the Klipperås study site shows a remarkable agreement between observed and predicted groundwater composition and offers an adequate description of the geochemical evolution of the aquifer. Proton fluxes are shown to be controlled mainly by calcite weathering and organic carbon degradation processes.

The impact of increased acidification is evaluated on the basis of various test cases and by including the soil compartment in the model framework. The results indicate that calcite weathering will be increased by a factor of two to three as a result of increased acidification. Furthermore, the calculations suggest that, once the powerful carbonate buffer is depleted, the buffer capacity is provided mainly by anaerobic respiration and ion exchange processes. Further ongoing acidic loading would lead to neutralization of alkalinity fluxes leaving the system with a very low buffering capacity towards fluctuations in proton fluxes.

Estimation of time scales of aquifer acidification was assessed under the focus of calcite depletion with aid of two acidification scenarios. These predict a time range of 12'400 to 370'000 years for calcite depletion to take place down to 500 meters depth. It is suggested from inherent model assumptions that these estimated time scales are conservative.

Table of materials

Table of materials (continued)

1 Introduction

Acid deposition has an increasing impact on the natural environment. Due to the combustion of fossil fuels, the natural balance between atmosphere, pedosphere and hydrosphere is disturbed in many regions. In southern Sweden, for example, the high acid load and the weak buffering capacity of the soil and subsoil has resulted in an increasing acidification trend of the shallow groundwaters (Brömssen, 1989).

The impact of acid atmospheric deposition on the pedosphere may induce the exceeding of the buffering capacity of the soil and lead to increased weathering. This effect is enhanced by the process of deforestation which occurs concurrently under severe conditions. In a previous report (Nebot and Bruno, 1991) we have studied these aspects on the basis of different scenarios and viewed the consequences of erosion with regard to the safety of a HLW repository. In this work we investigate the impact of soil acidification on the chemistry of the deep granitic groundwater and take the Klipperås study site as a test case. The goal is to explore the consequences of increased soil acidification on the geochemical stability of a HLW repository.

This study is presented in the following way. First, we introduce the acid neutralizing capacity concept and review the relevant processes consuming or producing acidity in aquifer systems. Then, after summarizing the geochemical and hydrological situation of the Klipperås area, we develop a geochemical model based on the STEADYQL algorithm (Furrer et al., 1989), which assesses the proton fluxes at steady-state in a granitic fracture system. From the imposed boundary conditions we apply the model to the present situation at Klipperås. We compare obtained results of groundwater composition with the measured levels and derive acidity and alkalinity fluxes. Furthermore, we model various test cases which represent different possible stages resulting from acidification and also include the soil compartment in the model. Thereof we derive the evolution of the aquifer affected by acidic influx. Finally, we assess time scales of acidification of the lower aquifer by critically viewing the uncertainties of geochemical and hydrological factors.

2 Concept of acid- and base neutralizing capacity

2.1 Definitions

The pH of natural waters is regulated by the acidity which in turn is determined by the dissolved species present. Thus, one needs to distinguish between proton concentration (or activity) as an intensity factor and the availability of protons, the H^+ reservoir, as given by the base neutralizing capacity (BNC). The BNC is equivalent to the total acidity or simply the acidity. The acidity, [Acy] (or H_{tot}), may be defined as the sum of the concentrations of all species containing protons in excess, minus the concentration of protons containing protons in deficiency with respect to a proton reference level. For natural waters the common reference level used is H_2O and H_2CO_3 (Schnoor and Stumm, 1985; Zobrist et al., 1987):

$$[Acy]^* = [H^+] + \upsilon[Al^{\upsilon+}] - [HCO_3^-] - 2[CO_3^{2-}] - [OH^-]$$

where υ $[Al^{\upsilon+}]$ depends on the speciation which depends on pH. The acid neutralizing capacity (ANC), or alkalinity [Alk] is defined as:

$$[Alk] = - [Acy] = [HCO_3^-] + 2[CO_3^{2-}] + [OH^-] - [H^+]$$

Considering the charge balance of the water, the acidity may be defined alternatively as:

$$[Acy] = 2[SO_4^{2-}] + [Cl^-] + [NO_3^-] - 2[Ca^{2+}] - 2[Mg^{2+}] - [Na^+] - [K^+]$$

$$= \Sigma[\text{conservative anions}] - \Sigma[\text{base cations}]$$

This means that any changes in the concentrations of cations or anions is accompanied by a shift in the acidity.

2.2 Processes affecting the H^+ balance in groundwater systems

Table 1 lists the main processes modifying the H^+ balance in groundwaters. Note that every process is expressed as stoichiometric reaction from which the change in acidity can be read from the H^+ per mole of reactant needed to balance the reaction.

---

* This definition neglects the contribution of weak acids (e.g., organic acids).

2.2.1 Weathering reactions

Chemical weathering reactions in groundwaters principally involve carbonate and silicate minerals. Dissolution of calcite, if present, is the main source of alkalinity. Weathering of silicates (feldspars, epidote, chlorite, micas) also leads to alkalinity increase. Contrary to carbonates, silicate dissolution is slow and kinetically driven; therefore, it strongly depends on hydrological conditions and on the nature of secondary precipitates (Drever and Zobrist, 1992; Velbel, 1985).

2.2.2 Ion exchange

Cation exchange occurs at the negatively-charged layer surfaces of phyllosilicates. Thus, in principle, protons may be exchanged for Na^+ or K^+. The relevance of proton exchange at neutral or slightly acidic conditions in clay systems (pH 4 - 6) is still controversial (Avena et al. 1990; Wieland pers. comm.). The process is also limited by the cation exchange capacity which, in the case of groundwater medium, is difficult to estimate. A further potential reaction involves the exchange of sulphate with surface-bound OH^- which occurs below pH 5 (Sposito, 1983) and decreases acidity.

2.2.3 Aluminium equilibria

Aluminium concentrations are predominantly controlled by gibbsite or kaolinite equilibria (see Table 1). Depending on the pH of the inflowing solution these minerals are dissolved or precipitated and thus the speciation of dissolved aluminium which strongly depends on pH is altered. Through this process buffering occurs between pH 4 to 6.

2.2.4 Redox processes

Table 1 lists some changes in the proton balance resulting from redox processes. Reduction reactions involve the microbially-induced interaction between organic matter and electron acceptors which lead to an increase in alkalinity. In most natural groundwaters iron oxides and sulphates are the dominant electron acceptors. The contribution of nitrogen via nitrification and/or denitrification may be significant in areas of high loads of acid deposition and of intense agriculture. In particular, loading of soil by airborne ammonia leads to increase of acidity via the nitrification process (Zobrist et al., 1987). Another oxidation process producing acidity involves sulphide oxidation (e.g., pyrite) with molecular oxygen.

Table 1 Main processes which modify proton balance

Weathering	
calcite	$CaCO_{3(s)} + 2H^+ <---> Ca^{2+} + H_2CO_3$
feldspar, e.g.,	$NaSi_3O_{8(s)} + H^+ + 7H_2O ---> Na^+ + 3H_4SiO_4 + Al(OH)_{3(s)}$
epidote (x = mole fract. Fe^{3+})	$Ca_2Al_{3-x}Fe_xSi_3O_{12}(OH)_{(s)} + 4H^+ + 8H_2O$ $---> 2Ca^{2+} + 3H_4SiO_4 + (3-x)Al(OH)_{3(s)} + xFe(OH)_{3(s)}$
Ion exchange	
proton exchange	$XNa + H^+ <---> XH + Na^+$
sulphate sorption	$2ROH + SO_4^{2-} <---> R_2SO_4 + 2OH^-$
Aluminium equilibria	
gibbsite	$Al(OH)_{3(s)} + 3H^+ <---> Al^{3+} + 3H_2O$
Redox reactions	
sulphide oxidation, e.g.,	$FeS_{2(s)} + {}^{15}/_4O_2 + {}^7/_2 H_2O ---> Fe(OH)_{3(s)} + 2SO_4^{2-} + 4H^+$
nitrification	$NH_4^+ + 2O_2 ---> NO_3^- + 2H^+ + H_2O$
sulphate reduction	$SO_4^{2-} + 2CH_2O + H^+ ---> HS^- + 2H_2CO_3$
iron oxide reduction	$Fe(OH)_{3(s)} + {}^1/_4CH_2O + 2H^+ ---> Fe^{2+} + {}^1/_4H_2CO_3 + {}^5/_2H_2O$
Mn(VI) oxide reduction	$MnO_{2(s)} + {}^1/_2CH_2O + 2H^+ ---> Mn^{2+} + {}^1/_2H_2CO_3 + H_2O$
denitrification	$NO_3^- + {}^5/_4CH_2O + H^+ ---> {}^1/_2N_2 + {}^5/_4H_2CO_3 + {}^1/_2H_2O$

<---> refers to fast reaction, ----> refers to slow reaction

3 The Klipperås study site

3.1 General

This site was investigated by SKB during the years 1984-1985. Main geological, hydrological, and geochemical results are reported by Olkiewicz and Stejskal (1986), Sehlstedt and Stenberg (1986), Gentzschein (1986), Tullborg (1986), Laurent (1986), Smellie et al. (1985; 1987), and Wikberg et al. (1987). A comprehensive summary of the Klipperås site investigations has been recently presented by Ahlbom et al. (1992). In the following only the major background information is given and special focus is addressed to the hydrological

and geochemical information and corresponding uncertainties which are used in the modelling section (section 4).

The Klipperås study site is located in Kalmar county (SE Sweden) about 35 km WNW of Kalmar. The larger area displays a flat topography, slightly dipping W-E. This direction also determines the surface water and regional groundwater flow. The ground is mainly covered with coniferous forest. The soil depth measured in the test site varies between 0.5 and 11 m, with mean value of 4.2 m (Smellie et al., 1987). The annual precipitation is around 760 mm, reflecting the relatively humid climate of southern Sweden.

3.2 Geology

Klipperås lies in the sub-Cambrian peneplain covered with Quaternary moraine deposits of several meters of thickness. Because of the scarcity of outcrops the main available geological information derives from cored drillings and surface geophysical surveys (Ahlbom et al., 1992). The bedrock underlying the moraine is mainly composed of granite, so-called Småland granite which constitutes 85% of the drilled rock volume. Further greenstone (7%) and different types and generations of dikes are found. These are composite dikes constituted of so-called Småland porphyries (5.5%), dolerite dikes (1.5%) and aplitic dikes (1%). The rock is strongly fractured. The fracture frequency is lowest for the Småland granite (4.3 fr/m) and highest for dolerite dikes (6.4-18.7 fr/m). Due to the limited geological data there are rather high uncertainties with respect to spatial distribution of rock types and of fracture zones as well as to the structural and tectonic interpretations.

3.3 Hydrology

The shallow groundwater system exhibits a low hydraulic gradient of about 0.5% from NW to SE. Due to the large uncertainties with regard to fracture zones only crude estimates of the hydraulic properties of the rock body have been performed. The hydraulic tests indicated a large scatter in hydraulic conductivity with a consistent decrease with depth (Gentzschein, 1986). Moreover, at a depth of 800 m a horizontal fracture zone with high conductivity ($2 \cdot 10^{-6}$ m/s) was observed. The estimated average effective hydraulic conductivity for the rock mass at 500 m depth are in the range of 10^{-9} m/s and are one to three magnitudes higher at shallow levels depending on the hydraulic model used (compare Lindbom et al., 1988 and Winberg and Gentschein, 1987). The hydraulic conductivity of the fracture zones at deep levels is estimated to be around 100 times the one of the rock mass. The applied hydrological models yield groundwater flow rates ranging from 40 - 300 mL/m^2/yr at a depth of 500 m.

In general, the calculated effective hydraulic conductivity and flow rates are significantly higher than the ones calculated in other SKB sites, such as Fjallveden, Gidea, Svartboerget, and Kamlunge.

3.4 Geochemistry

3.4.1 Deep groundwaters

Within the Klipperås test site programme the geochemistry of some deep level groundwaters in combination with hydraulic tests was investigated (Smellie et al., 1985; 1987; Laurent, 1986; Wikberg et al., 1987). Table 2 lists composition of representative groundwaters for which contamination due to the drilling procedure is considered negligible. Also, the fracture-filling minerals encountered in the analyzed fracture zones and estimated hydraulic conductivities are indicated (Table 3). The major-ion chemistry reveals that there is relatively little variation in composition. All waters are of rather low salinity with the predominance of Na^+, Ca^{2+}, and HCO_3^-. According to the major composition all waters are of near-surface and intermediate origin (Smellie et al., 1987) and no deep saline-rich varieties were found. Environmental isotope data indicate that groundwaters are of meteoric origin. Another typical feature of the deep groundwaters is their low redox potential, also reflected by the measurable Fe(II) and sulphide content and low sulphate concentrations.

Table 2 Major ion composition of representative deep groundwaters at Klipperås (Smellie et al., 1987) Groundwaters where contamination due to sampling procedure has occurred are not given here.

borehole no.	depth m	pH	Na^+ mM	Ca^{2+} mM	Mg^{2+} mM	K^+ mM	HCO_3^- mM	Cl^- mM	SO_4^{2-} mM
KKL02	326	7.6	1.26	0.76	0.041	0.028	2.29	0.48	0.001
KKL01	406	8.3	2.04	0.34	0.095	0.026	1.31	1.27	0.016
KKL09	696	7.6	0.65	0.71	0.12	0.033	1.97	0.17	0.045

Calcite was observed in all fractures associated with the extracted waters. This observation is consistent with the fact that the waters are close to saturation with respect to calcite. A detailed study on the mineralogy of fractures (Tullborg, 1986) shows that for the great majority of fractures at deeper levels calcite is the dominant mineral, whereas the upper part shows depletion with regard to carbonates. Other fracture minerals include chlorite, epidote, ferric oxide, clay minerals, gibbsite, and occasionally siderite and pyrite (Table 3).

Table 3 Redox sensitive parameters of deep groundwaters at Klipperås.

borehole no.	depth m	E_H mV	Fe(II) µM	S(-II) µM	NO_3^- µM	NH_4^+ µM	TOC mg/L
KKL02	326	-290	2.32	3.11	1.42	2.50	2.0
KKL01	406	-300	0.14	2.81	0.36	0.72	3.7
KKL09	696	-270	1.61	0.32	1.42	1.42	1.2

In general, the data suggest a gradual evolution of dilute meteoric water by mineral-water interactions, anaerobic respiration and ion exchange processes through a downward hydraulic gradient. This is supported, e.g., by the distribution pattern of calcite in the fractures and by the evidence of anaerobic respiration processes. The relevance of mixing with groundwater of different sources cannot be elucidated with the available data (cf. Smellie et al., 1987). Ahlbom et al. (1992) suggest the presence of old glacial melt water at depth.

Table 4 Fracture minerals and hydraulic conductivities of fracture zones.

borehole no.	section	minerals	K-values m/s
KKL02	328-331 m	chlor-cc-epi	$4.7\ 10^{-10}$
	623-628 m	chlor-cc-Fe(III)ox-(sid)-(gibb)-(kao)	$5.5\ 10^{-10}$
	741-746 m	cc-chlor-musc-Fe(III)ox	$8.2\ 10^{-9}$
	792-804 m	cc-chlor-Fe(III)ox-pyr-(epi)	$1.2\ 10^{-6}$
	865-870 m	epi-chlor-cc	$6.9\ 10^{-9}$
KKL01	25-30 m	Fe(III)ox-chlor	not tested
	280-295 m	clor-cc-(Fe(III)ox)	$9.3\ 10^{-7}$
	450-564 m	chlor-cc- epi- musc- (kao)- (gibb)	$6.6\ 10^{-10}$
KKL09	120-160 m	chlor-cc-qz-Fe(III)ox	$5.4\ 10^{-7}$
	615-665 m	clay-Fe(III)ox	$3.1\ 10^{-10}$
	696-701 m	chlor-musc-epi-sid-gibb-goe	$9.4\ 10^{-8}$

Fe(III)ox: ferric oxides; chlor: chlorite; cc: calcite; epi: epidote; musc: muscovite; kao: kaolinite; gibb: gibbsite; sid: siderite; pyr: pyrite; clay: clay minerals; goe: goethite

3.4.2 Shallow groundwaters

The shallow groundwaters in the Klipperås area have not been investigated in the SKB studies. However, there are a number of data available concerning the shallow aquifers in the area around Klipperås (Knutsson, 1970; Knutsson, 1971; Jacks and Knutsson, 1981) since many of them are used for local water supply. Most groundwater analyses have been derived from the moraine which is mainly constituted of coarsely grained till soil whereas some data reflect samples of the underlying rocks (granite, porphyry, and greenstone). Table 5 gives the

range of major composition of 32 groundwaters extracted from forested springs and wells near Emmaboda (Jacks and Knutsson, 1981), about 10 km south of Klipperås. This shows that these waters are very low in dissolved salts, as also indicated by the low electrical conductivity which is found to be 3-10 mS/m. Moreover, the waters are low in alkalinity and display CO_2 contents of 0.5-2 % of the soil atmosphere. Some of the spring waters which generally reflect short residence times (weeks to months) in the soil are slightly acidic as will be further outlined in the next section.

Table 5 Range of major composition and estimated average of 32 forest wells and springs extracted in Kalmar County (Jacks and Knutsson, 1981).

	Na^+ mM	Ca^{2+} mM	Cl^- mM	SO_4^{2-} mM	HCO_3^- mM	Al mM	pH
minimum	0.10	0.10	0.06	0.10	0.00	0.002	4.2
maximum	0.30	0.50	0.20	0.25	0.30	0.27	6.8
est. average	0.20	0.20	0.14	0.20	0.15	0.005	5.8

3.5 Acidification trends

Acid precipitation in southern Sweden has strongly increased since the late fifties (Rohde and Granat, 1984), although since the eighties a decrease due to lower SO_2 emissions has been noted (Brömssen, 1989). A further general increase for the next 300 years is expected, whose extent depends on the climatic scenario invoked (Hordijk et al., 1989; Nebot and Bruno, 1991). As a result of acid precipitation, sulphate in shallow groundwaters has increased notably. In some areas in southern Sweden the acidity input has exceeded the buffering capacity of the soil and a significant drop in pH has been noted (Brömssen, 1989). In Kalmar county (vicinity of Emmaboda) an acidification trend between 1964 and 1980 was observed from forest well and spring analyses (Jacks and Knutsson, 1981), which show an increased total hardness/alkalinity ratio between 1964 and 1980.

The extent of acidification in Kalmar County is illustrated by the acidity of some soil waters which were extracted from three springs and one well (Jacks and Knutsson, 1981). Table 6 shows the major composition of these waters. Also, the estimated composition of the rain and/or snow water using chloride as conservative tracer is given. This indicates that interaction with the soil matrix results mainly in Al and Si release, whereas the other components are not much affected. Thus, it appears that the ANC capacity of the soil is very

limited in some parts of the area and is provided mainly by weathering of Al and Si bearing minerals.

Table 6 Composition of some acidified soil waters and estimated composition of atmospheric water (rain/snow) (from Jacks and Knutsson, 1981).

	Na^{2+} mM	Ca^{2+} mM	Cl^- mM	SO_4^{2-} mM	HCO_3^- mM	SiO_2 mM	Al mM	pH
Tallebo spring	0.18	0.09	0.19	0.16	0.00	0.12	0.27	4.2
atmosphere	0.21	0.19	0.19	0.30	0.00	0.00	0.00	
Etskogen well	0.08	0.06	0.06	0.11	0.00	0.07	0.02	4.5
atmosphere	0.07	0.06	0.06	0.09	0.00	0.00	0.00	
Peppar spring	0.25	0.11	0.17	0.24	0.01	0.13	0.01	4.8
atmosphere	0.19	0.17	0.17	0.27	0.00	0.00	0.00	
Margareta well	0.21	0.14	0.14	0.20	0.15	0.00	0.00	5.4
atmosphere	0.16	0.14	0.14	0.22	0.00	0.00	0.00	

4 The model

4.1 General concept

The effect of acid precipitation on a granitic aquifer is schematically shown in Fig. 1. In a general view, it can be regarded as a two-step process involving (1) the interaction of the acidity with the forest and soil system and (2) the interaction of the shallow groundwater with the granitic bedrock system. The first process, which has been extensively investigated over the past years (e.g., Ulrich et al., 1980; Ulrich, 1981; Schnoor et al., 1984), mainly includes biomass synthesis (aggrading forest) and soil weathering (Schnoor and Stumm, 1985; Driscoll and Likens, 1982) whose balance is affected by acid precipitation. As a result the soil solution, surface water, and shallow groundwater may become acidified when the ANC of the soil system is exceeded. Thus, the second process is an imprint of the H^+ buffering capacity of the overlying soil. The ANC of the granitic aquifer is determined on one hand by the weathering of primary and secondary minerals and oxidation of organic matter and by the hydraulic conditions on the other.

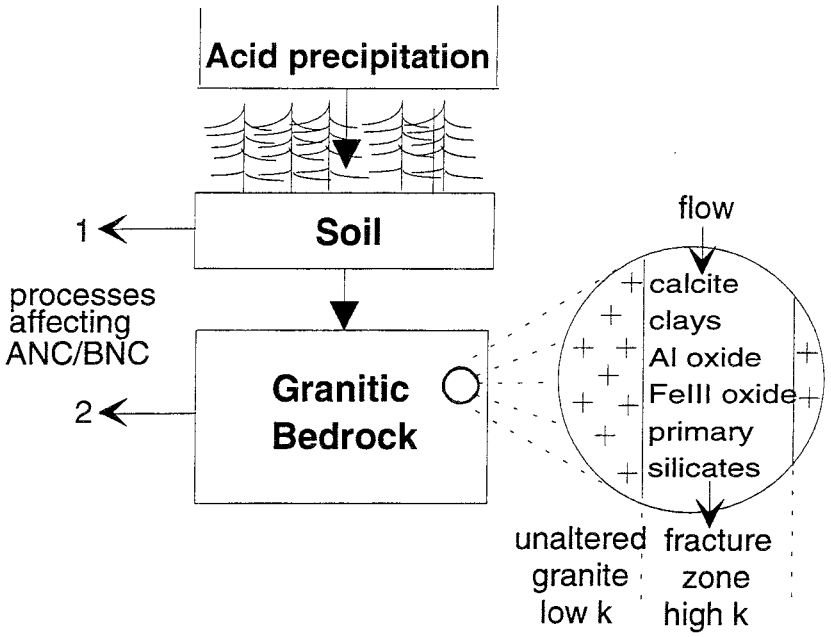

Fig. 1 Simplified concept of acidification for a granitic aquifer system. Processes affecting acid neutralizing capacity (ANC) and base neutralizing capacity (BNC) processes can be viewed in the soil and in the granitic bedrock compartment separately (see text). "k" refers to hydraulic conductivity.

Various models have been used to predict the influence of acidic precipitation on aquatic systems. In the "trickle-down" model (Schnoor et al., 1984; Nikolaidis et al., 1988) changes of alkalinity in surface water, soil water, and groundwater resulting from different chemical and biological processes are quantified using a single parameter approach for transfer between compartments. In the "Rains" model (Horjik et al., 1989) predictions of acid loads on the environment are assessed based on climatic scenarios. Other models have focused on the chemical and hydrological processes affecting soil acidity; e.g., the "Magic" model (Cosby et al., 1986) or the ILWAS model (Integrated Lake Water Acidification Study: Gherini et al., 1985; Davis et al., 1987). In a recent study Furrer et al. (1990) used a relatively simple, yet mechanistic model based on the STEADYQL algorithm to describe interactions among soil solids, biota, and atmosphere and to predict acidity in forest soils. In this work we apply the STEADYQL approach to the prediction of deep groundwater composition resulting from acidic inflow (process (2), see above) in the Klipperås area. Thus, this progress report focuses on the acidity/alkalinity fluxes within the granitic aquifer arising from realistic inflow solutions. Subsequently, the modelling approach is extended by including the overlying soil compartment.

4.2 Description of the model

4.2.1 Geochemical and hydrological boundary conditions

In our model we consider a hypothetical volume element of the fractured granitic bedrock through which groundwater moves downwards (cf. Fig. 1). The boundary conditions for this compartment are imposed by (1) the hydraulics, (2) interaction of the solution with primary and secondary minerals, (3) decomposition of organic matter by microbial activity, (4) the composition of inflowing solution. A schematic presentation of the processes which influence the groundwater composition is given in Fig. 2. Furthermore, in the first stage of model testing, we do not take mixing of different water qualities into account. From the available hydrological and geochemical data (section 3) we attempt to define these boundary conditions within the framework of the STEADYQL modelling approach.

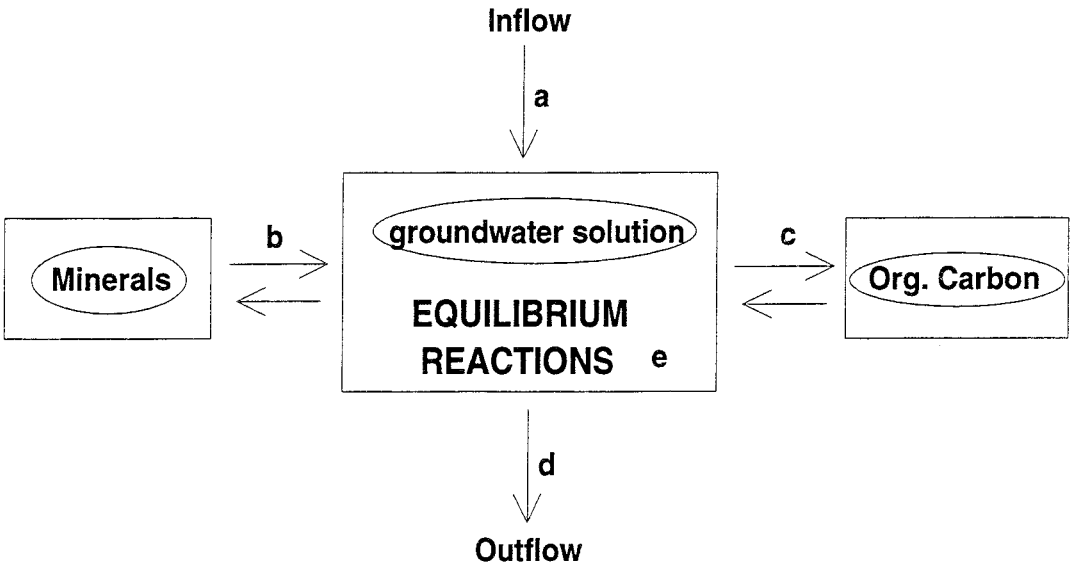

FLUXES

a	Shallow groundwater composition (outflow from soil compartment)
b	Weathering and precipitation of minerals (not in equilibrium with solution)
c	Aerobic and anaerobic respiration: O_2, sulphate, Fe(III) reduction, denitrification
d	Outflow of deep groundwater
e	Complex formation in solution, ion exchange at mineral surfaces, solubility equilibria

Fig. 2 Processes which influence composition of groundwater (modified from Furrer, 1991).

Hydraulic conditions: In the STEADYQL approach water movement is presented as average flow velocity. In a highly fractured granitic medium such as Klipperås flow predominantly occurs through fracture zones whose hydraulic conductivity is around 50 - 100 times higher ($\approx 10^{-8}$ - 10^{-6} m/s) than in the whole rock mass (Ahlbom et al., 1992). The estimated average flow velocity in the rock mass, as calculated by hydrogeological models, is around 60 - 300 mL/m^2/yr at 500 m depth and 300 - 3000 mL/m^2/yr in the upper part depending on the models used (Lindbom et al., 1988; Winberg and Gentschein, 1987). Thus, we take the average flow velocity of the fracture zones (between 0 - 500 m depth) to range between 4.5 - 225 L/m^2/year or 0.0045 - 0.225 m/yr. In addition, the effect of highly permeable fractures which are also encountered in fractured granitic rocks (SKB-91) is considered, taking a high flow velocity of 3.17 m/yr.

Mineral-water interactions: The relevant mineral-water interactions are identified by their historical record as given by the nature of fracture filling minerals (Table 4) and by the water composition (Table 2 and 3). Here we are principally interested in the processes that neutralize or produce acidity. Calcite weathering

$$CaCO_3(s) + 2H^+ <---> Ca^{2+} + H_2CO_3 \qquad (1)$$

is the dominant process controlling alkalinity as revealed from the abundance of this mineral in fracture zones and the composition of deep groundwaters which are roughly in equilibrium with respect to calcite (Smellie et al., 1987). The identification of gibbsite precipitates (Tullborg, 1986) in a number of locations suggests equilibrium with respect to this aluminium (hydr)oxide phase:

$$Al(OH)_3(s) + 3H^+ <---> Al^{3+} + 3H_2O \qquad (2)$$

The frequent presence of ferric oxides appears to indicate equilibrium conditions with regard to this phase. On the other hand, the measured redox potentials suggest that the solutions are not in equilibrium with respect to the Fe^{3+}/Fe^{2+} couple (Wikberg et al., 1987). In the STEADYQL modelling approach this apparent controversy is not relevant because reductive dissolution of ferric oxides is treated as kinetic process (see following section).

Silicate weathering is another source of alkalinity. Primary silicate minerals include mainly feldspars, biotite, and quartz, identified secondary silicate minerals include chlorite, epidote, clay minerals. Generally, alkaline minerals such as plagioclase weather faster than acidic ones (K-feldspar, quartz, biotite) or stable weathering products (Velbel, 1985). Therefore, as an

upper limit for alkalinity production, we consider albite (Na-plagiocase) weathering (Banwart et al., 1994). The incongruent dissolution of albite can be expressed as

$$NaAlSi_3O_{8(s)} + 7H_2O + H^+ \text{ ---> } Na^+ + 3H_4SiO_4 + Al(OH)_{3(s)} \quad (3)$$

Ion exchange reactions involving clay minerals (kaolinite, illite, smectite) may also provide a buffer to acidic influx. Such reactions mainly occur at the permanently charged layer sites which are defined by the cation exchange capacity (CEC). The cationic displacement of the main counter ion by other ions, I (H^+, K^+, Ca^{2+}) is schematically expressed as

$$zXNa + I^{z+} \text{ <---> } X_zI + zNa^+ \quad (4)$$

where X is the exchangeable site at the clay surface and z is the charge of the ion I.

Oxidation of sulphides constitutes a process for production of acidity. Pyrite has been identified as fracture-filling mineral in some locations (Tullborg, 1986). Pyrite surfaces show high reactivity with regard to molecular oxygen and oxidize to ferric oxides.

$$FeS_{2(s)} + {}^{15}/_4O_2 + {}^7/_2 H_2O \text{ ---> } Fe(OH)_{3(s)} + 2SO_4^{2-} + 4H^+ \quad (5)$$

Decomposition of organic matter: The presence of considerable levels of total organic carbon (≈ 1-4 mg/L, Table 4) and the relatively high p_{CO_2} levels in the deep groundwaters of Klipperås indicate that respiration processes are important. From the composition of the water and from general information on granitic groundwaters (e.g., Banwart et al., 1992; Wikberg et al., 1987), the main electron acceptors involved in the oxidation of carbon are molecular O_2, ferric iron, and sulphate:

$$O_2 + CH_2O \text{ ---> } H_2CO_3 \quad (6)$$

$$Fe(OH)_{3(s)} + {}^1/_4CH_2O + 2H^+ \text{ ---> } Fe^{2+} + {}^1/_4H_2CO_3 + {}^5/_2H_2O \quad (7)$$

$$SO_4^{2-} + 2CH_2O + H^+ \text{ ---> } HS^- + 2H_2CO_3 \quad (8)$$

Studies on redox processes performed at the Äspö Hard Rock Laboratory indicate that organic carbon is the major source of electrons for electron acceptors, including molecular O_2 (Banwart et al., 1992) and therefore aerobic respiration (Eq. 6) will likely predominate over pyrite oxidation (Eq. 5) with regard to O_2 fluxes.

The frequent occurrence of ferric oxides as fracture-filling minerals at all sampled depths indicates that Fe(III) is an important electron acceptor but gets reduced at a relatively slow rate in the anoxic groundwater system. The slow reductive dissolution of ferric oxides both by biotic and abiotic means has been demonstrated experimentally (Lovley, 1987; LaKind and Stone, 1988) and in the field (Canfield, 1990; Wersin et al., 1991). The low concentrations of sulphate in the deep groundwaters and the relatively elevated levels of dissolved sulphide (Tables 2 and 3) indicate that biologically-mediated reduction of sulphate is significant.

The relatively low concentrations of Fe(II) observed in the groundwaters suggest a sink for this component by secondary precipitation. Siderite has been observed in some locations, however groundwater compositions exhibit significant undersaturation with regard to this mineral (Smellie et al., 1987). On the other hand the similar levels of dissolved Fe(II) and HS^- are compatible with the formation of iron sulphide:

$$Fe^{2+} + HS^- \text{ <---> } FeS(s) + H^+ \qquad (9)$$

The solubility of FeS depends largely on the crystallinity of the precipitate. The observed concentrations indicate that groundwaters are close to equilibrium with respect freshly precipitated FeS (Berner, 1981). This suggests that precipitation of FeS is an active process.

The low concentrations of nitrogen compounds (<5 μM N_{tot}) in the deep groundwaters reveal that denitrification or nitrification play a minor role in the production or consumption of alkalinity. Similarly, the absence of manganese oxides in the mineralogical investigations (Tullborg, 1986) indicates that reduction of Mn(III, IV) is not significant.

Composition of inflowing solution: In our modelling concept the solution composition of the inflow in the granitic fracture zone represents the very shallow groundwater or soil water which has been affected by the acid load. Thus, the appropriate constraints on the average composition of this water are critical for assessing the effect of acidification on the deeper groundwater. Here we will follow a two-step procedure. First, the present situation will be modelled (section 4.3) with aid of the approximate composition of the shallow medium (given as average composition in Table 5). The water composition taken from the forest wells indicates a dilute, slightly acidic water, undersaturated with respect to calcite. This agrees with the mineralogical observations which indicate the lack of calcite at the shallower levels of the fractures (Tullborg, 1986). Moreover, although no aluminium data is reported, we assume gibbsite equilibrium which is known to control Al levels in most soil and shallow groundwaters (Appelo and Postma, 1993) at pH values above 4.5 and provides an important buffer to alkalinity/acidity fluctuations at acidic to neutral conditions. The second step

involves the estimation of future inflow compositions arising from increased acid load by assuming various test cases of different inflow acidity. In the third step we will include the soil compartment and assess the influence predicted acid deposition rates on deeper groundwaters.

4.2.2 Application of the STEADYQL approach

The STEADYQL code is very versatile with regard to defining the geochemistry of the system of interest. Fluxes within the system are viewed under the focus of long time scales. Chemical reactions that produce or consume acidity are treated as fast or slow processes.

Fast processes are treated as equilibrium reactions. In the present case this includes (a) fast mineral-water interactions, such as dissolution of calcite, dissolution of gibbsite, precipitation of iron sulphide (b) acid-base and complexation reactions within the groundwater. Ion exchange at clay surfaces is also fast. This process is expected to significantly contribute to the increase of Na^+ in granitic groundwaters (Banwart et al., 1992) (Eq. 4). In the present version of STEADYQL this type of process is not taken into account because all surface processes are regarded under the constraint of steady-state which means that the solution composition of the modelled volume is not affected by surface reactions. In view of this, we approximate the sodium exchange process by considering it as ligand exchange reaction (Wanner, 1986) and estimating the cation exchange capacity (CEC), as outlined in section 4.3.1.

Slow processes are described with rate equations and rate constants and include all other processes contributing to acidity/alkalinity production. These are oxidation of organic matter by O_2, Fe(III) and sulphate reduction, silicate weathering, and pyrite oxidation. Furthermore, inflow of acidic solution is viewed as slow process. Because of the large uncertainties with regard to a number of critical factors, such as hydraulic conditions, mineral surface areas, and biological activity, we assign a zero-order rates for each of these slow reactions. The estimation of the rate constants is assessed in the following manner

- Silicate weathering: Albite weathering (Eq. 3) is selected as upper limit for alkalinity production (cf. section 4.2.1). According to Knauss and Wolery (1986) dissolution of fresh albite at neutral conditions yields a rate of $6 \cdot 10^{-7}$ mole Si m^{-2} wk^{-1}. From experimental data derived from the Äspö Hard Rock Laboratory Banwart et al. (1992) estimated an upper limit of wetted surface area of about 10 m^2 L^{-1} and an upper porosity of the rock mass of $2 \cdot 10^{-4}$. Using these values we obtain $k_{Alb} = 1 \cdot 10^{-13}$ mole L^{-1} s^{-1}.
- Aerobic respiration: The kinetics of this process strongly depend on the reactivity of the organic matter and hydrological conditions. Results from the Äspö study indicate fast

depletion of O_2 in a granitic aquifer. For simplicity we assume pseudo zero-order reaction, then by estimating a dissolved O_2 concentration in the aerated soil of about 0.1 mM, we obtain, from an imposed flow of 10^{-9} m/s, a rate constant: $k_{O_2} = 10^{-12}$ mole L^{-1} s^{-1}.

- Reductive dissolution of Fe(III): The kinetics of reductive dissolution of ferric oxides (Eq. 7) have shown to be surface-controlled (Sulzberger et al., 1989; LaKind and Stone, 1988) and to follow pseudo zero-order kinetics. From field investigations on anoxic lake sediments (Wersin et al., 1991) the rate of Fe(III) transformation has been estimated to be about 10^{-12} mole Fe per L porewater and seconds. Assuming that reactive surface area of ferric oxide per L of water in a granitic fracture zone is similar or lower, we estimate a range for the kinetic constant to be $k_{Fe(III)} = 5 \cdot 10^{-13} - 5 \cdot 10^{-12}$ mole L^{-1} s^{-1}.

- Sulphate reduction: An assessment of the redox kinetics of sulphur (Eq. (8)) is difficult mainly because of the large uncertainties concerning the nature of organic matter and biological activity involved in sulphate reduction. However, the reduction rate is constrained by the fixed activity of reduced sulphur via FeS precipitation (see following section).

4.2.3 Coupling of iron and sulphur cycles

In the modelling concept the fluxes of iron and sulphur are coupled via iron sulphide precipitation (Eq. 9). Combining this equilibrium reaction with Eqs. (7) and (8) we obtain:

$$^{9}/_{4}CH_2O + 2H^+ + SO_4^{2-} + Fe(OH)_{3(s)} \text{ ---> } ^{9}/_{4}H_2CO_3 + FeS_{(s)} + ^{10}/_{4}H_2O \qquad (10)$$

This implies that the Fe(III) and SO_4^{2-} reduction processes are coupled and that

$$k_{FeIII} = k_{sulf} \qquad (11)$$

4.2.4 Definition of steady-state condition

At steady-state the fluxes of each chemical component balance out, which means that the sum of all fluxes entering the volume compartment are exactly compensated by the ones leaving it. Therefore, at steady-state the outflowing solution has the same composition as the one of the modelled compartment. The system is defined by the mass action equations, the kinetic rate expression and the rate constants. The principles of the algorithm are extensively described in Furrer et al. (1989).

4.3 Modelling present situation

4.3.1 "Calibration" of system

The purpose of this exercise is to validate the proposed model which should predict the composition of the deep groundwater from the imposed input parameters. These are constrained by the laws of mass action, equilibrium constants, the estimated inflow composition, and the imposed flow velocity. However, the kinetic rate constants of the slow redox processes including aerobic respiration, Fe(III) reduction, sulphate reduction are not precisely known for the modelled system. Preliminary calculations showed that the system is very sensitive to these variables which strongly depend on the flow velocity. Therefore, we vary these variables for a given flow velocity under the condition imposed by Eq. (10) in order to determine the "operational" zero-order constants of the system. These constants are then compared to realistic kinetic constants, as outlined above. In the modelling procedure it is convenient to define a reference case which is based on realistic estimates of the geochemical variables. The validity of these estimates is then checked by a sensitivity analysis in which the uncertainties within the assumed values is taken into account. In this case we will, after presenting the results obtained for the reference case, assess the influence of flow, inflow composition, and mixing of different waters (section 4.3.3).

Inflow: The inflow composition of a realistic average shallow groundwater has been estimated, by taking the average major composition of forest springs and wells, as given in Table 4. A representative p_{CO_2} from the measured soil air (Jacks and Knutsson, 1981) is $\approx$ 0.01 atm. Dissolved O_2 has not been reported; it is estimated to be about 0.1 mM. [Fe(II)] and [HS^-] are assumed to be below 10^{-9} M. Furthermore, gibbsite equilibrium is assumed. Equilibrium modelling is performed with the MICROQL code (Westall, 1986) which yields the speciation of the inflow solution.

Ion exchange: The increase of Na in the deeper groundwater can be largely explained, in the absence of significant mixing processes, by NaCl dissolution and ion exchange reactions. Preliminary calculations indicated that silicate dissolution (e.g., albite, Eq. 3) is of minor importance in this regard because of its slow weathering kinetics. Compositions at Klipperås (Table 2) reveal that Na^+ is in excess relative to Cl^- by a factor of $\approx$ 2. In view of this, we suggest that this difference is caused by Na-Ca exchange at clay surfaces. From this and under the assumption of ideal exchange behavior (Sposito, 1983) a crude estimate of the exchangeable sites can be made. Taking an average concentration of Na^+ of 1.3 mM and attributing half of the increase (1 mM) to ion exchange an amount of $\approx$ 1 meq/L of exchangeable sites is obtained.

Flow velocity: The average flow velocity in the fracture zones is estimated to roughly vary between 10^{-8} and 10^{-10} m/s. As a reference case we assume an intermediate flow velocity of 10^{-9} m/s.

With these additional geochemical specifications the system is defined and the model can be run and validated by comparing the results with the measured groundwater composition.

4.3.2 Results for reference case

Table 6 shows obtained steady-state concentrations of the modelled volume (fracture zone). Also, the average concentrations and standard deviations derived from the three representative groundwaters are given. A comparison with the modelled results shows that they are very similar to the actually measured concentrations. All concentrations of major components are within the standard deviation of the three selected representative deep groundwater samples. This results indicates that the applied STEADYQL approach predicts the geochemical evolution of the major components of the groundwater reasonably well.

Table 6 Average composition of deep groundwaters (KKL01, KKL02, KKL09) with standard deviation (measured) and the predicted one with STEADYQL approach (model).

	pH	Na^+ mM	Ca^{2+} mM	HCO_3^- mM	Cl^- mM	SO_4^{2-} mM	Fe(II) µM	S(-II) µM
measured	7.8	1.30±0.70	0.60±0.23	1.86±0.50	0.64±0.57	0.021±0.02	1.36±1.11	2.08±1.53
model	8.0	0.98	0.64	1.40	0.66	0.010	1.49	2.66

Redox rates: As mentioned in the above section, the selection of the rate constants associated with redox processes is found to be a critical step in the modelling procedure. The selected values for the assumed zero-order reactions are:

Aerobic respiration (Eq. 6): $k_{O_2} = 1.00\ 10^{-12}$ mole L^{-1} s^{-1}

Ferric oxide reduction (Eq. 7): $k_{FeIII} = 1.95\ 10^{-12}$ mole L^{-1} s^{-1}

Sulphate reduction (Eq. 8): $k_{sulf} = 1.95\ 10^{-12}$ mole L^{-1} s^{-1}

Calculations showed that these three redox processes are sufficient to describe the system. As a test, the reduction of O_2 by reaction with pyrite was included instead of aerobic respiration. Similar results in term of proton fluxes and p_{CO_2} were obtained. The optimal rate found for reductive dissolution of ferric oxide is in the range of the ones estimated in anoxic sediments

($2 \cdot 10^{-13}$ - $5 \cdot 10^{-12}$ mole L^{-1} s^{-1}, section 4.3.1). This good consistency of the obtained "operational" kinetic constants suggests that the assumed average flow velocity, v, of 10^{-9} m/s is a reasonable upper estimate, independently of the hydraulic data, since the chosen constants are closely linked to this parameter. Thus, a decrease of v by a factor of 10 implies the same decrease of the kinetic rate constants in order to obtain the same solution composition. In summary, the obtained rate constants for ferric oxide dissolution are compatible with a flow velocity of 10^{-10} - 10^{-9} m/s.

Proton fluxes: The relative contribution of each process in affecting the flux of H^+, or the change in alkalinity is illustrated in Fig. 3. The flux is expressed in equivalents alkalinity or acidity per L of groundwater and year. The largest contribution to the alkalinity flux arises from weathering of calcite fracture minerals. This process, however, is strongly influenced mainly by the considered redox processes. Thus, biologically-mediated reduction of sulphate and Fe(III) produce increase in alkalinity and p_{CO_2}. On the other hand, precipitation of ferrous iron provides a sink for alkalinity. Note that aerobic respiration does not influence alkalinity/acidity fluxes. STEADYQL calculations show that redox processes must be invoked to explain the resulting pH and alkalinity that is observed in the deep groundwater. Neglecting these redox processes in the calculations leads to unrealistically high pH ($\approx$ 10) and low p_{CO_2}. It must be pointed out, however, that this statement only holds when the lower aquifer is closed with respect to CO_2 exchange. This assumption appears reasonable since the relatively high CO_2 flux from the overlying soil compartment will be dispersed to a large extent in the large granitic reservoir. Nevertheless, we have run calculations at an imposed constant p_{CO_2} in the range of the one observed in the deep groundwaters and lower rates of sulphate/Fe(III) reduction. These results indicate that similar composition is reached except for observed sulphate concentrations which are too high compared to observed levels. This further supports the validity of the selected geochemical boundary conditions.

The results indicate that weathering of silicates does not provide a significant alkalinity flux in the studied groundwater system. This is consistent with modelling studies performed within the Äspö Hard Rock Laboratory (Banwart et al., 1992). Fluxes involving aluminium do not notably affect alkalinity. Cation exchange at clay surfaces does not have a direct influence on alkalinity fluxes. However, our results show that calcite weathering is increased (ca. 4%) due to simultaneous Na-Ca exchange:

$$2XNa + CaCO_3 + H^+ <---> X_2Ca + HCO_3^- + 2Na^+ \qquad (12)$$

As mentioned in the above section, the ion exchange processes occurring at clay surface layers have been modelled on the basis of the observed increase of Na^+ with depth (Eq. 4).

This implicitly implies that the distribution of cations (mainly Na/Ca) changes with time. Therefore, this representation of ion exchange implies a transient rather than a steady-state behavior. At steady-state the solution composition is independent of fast (equilibrium) surface reactions. This shows an important limitation of the steady-state assumption. In view of this, we have approximated ion exchange as ligand exchange reactions in solution assuming an initial distribution of Na/Ca of 1.5 and a cation exchange capacity (CEC) of 1 meq/L (see above section). We are aware that this approximation is arbitrary. We are presently in the process of including the possibility of transient behavior of surface reactions into the STEADYQL code.

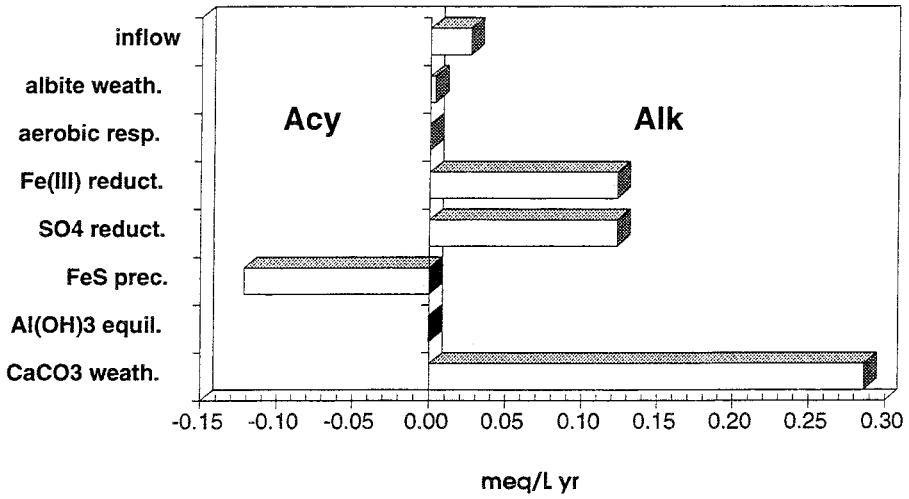

Fig. 3 Modelling present situation. Alkalinity (+) and acidity (-) fluxes caused by chemical processes and inflow. Flux due to outflow (not presented) accounts for difference between presented alkalinity and acidity fluxes.

Summary: The results obtained from STEADYQL show that the imposed boundary conditions are adequate and allow prediction of the chemical composition of the deep groundwater. The relevant processes contributing to alkalinity fluxes are in the order of their importance: calcite dissolution, sulphate reduction/ferric oxide reduction, and Na-Ca exchange. Acidity fluxes are induced by precipitation of ferrous sulphide. The kinetic constants used for the redox processes are consistent with previous kinetic data from experimental and field observations. The obtained fluxes are directly related to the selected average flow velocity of 10^{-9} m/s. The overall consistency obtained by the model suggests

that this estimate is appropriate in spite of the large uncertainties regarding hydraulics of the deep groundwater system. The modelling of ion exchange process has been done in a preliminary way due to large uncertainties in the CEC and because of the probable transient rather than steady-state behavior of this process.

4.3.3 Sensitivity analysis

In order to assess the sensitivity of the proposed model, we have run additional calculations by taking into account the uncertainties of the input variables assigned to the reference case, as defined above. In particular, the effects of inflow composition, flow conditions, and mixing of different waters on the model predictions have been studied.

Inflow composition:

The effect of deviations from the estimated average composition of the soil water has been evaluated by taking into account the range of major ion concentrations from well and spring analysis (Table 5). Fig. 4 shows the influence of changing concentration (or activity) on the predicted Ca in solution (and thus on the flux of weathered calcite). The results are presented in the form as relative variations with regard to the reference case (factor f). Thus, a factor f = 2 represents a two-fold increase in concentration with regard to the average concentration. Note that the filled circle shows the result for the reference case. The dashed lines refer to the observed range of Ca concentrations in the deep groundwaters. The results indicate that, in general, model predictions, are not largely affected by realistic variations in the inflow composition. Thus, increase of proton concentrations (or decrease of pH) at constant p_{CO_2}, or increase of Ca^{2+}, SO_4^{2-}, or O_2 leads to only slight changes in the predicted compositions and are within the range of the one observed. Increase in inflow pH to a value above 6.3 induces a decrease in calcite dissolution. A much stronger effect on the end composition arises from variations in p_{CO_2}. The effect of CO_2 on alkalinity fluxes will be further discussed in section 4.4. However, we would like to point out here that the model suggests that an inflow p_{CO_2} of around 0.01 atm is a reasonable upper estimate for shallow groundwaters of the Klipperås area. This is also consistent with measurements of soil air compositions (cf. Jacks and Knudsson, 1981).

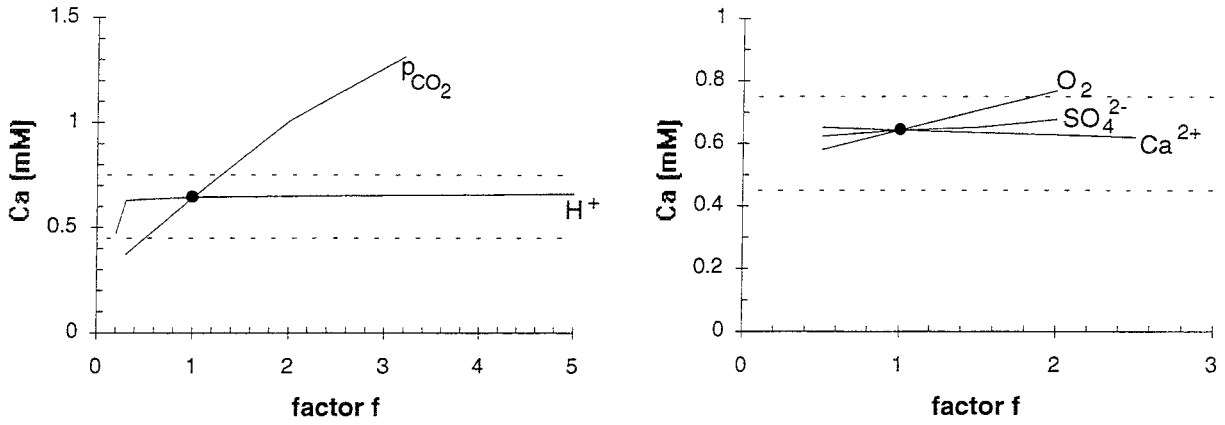

Fig. 4 Sensitivity analysis of major inflow parameters. The factor f refers to the variation with regard to the reference case (f = 1), indicated by filled circle. Dashed lines give range of observed concentration of Ca in the deep groundwater.

Flow conditions:

As discussed above, the component fluxes are closely related to the flow velocity, v. In the case of fast chemical processes, at steady state, fluxes are linearly dependent on v. For slow chemical processes, such as redox processes, there is no simple relationship between v and fluxes and therefore we have estimated rates of transformation for a reference case. The fact that the obtained rate of ferric oxide weathering agrees fairly well with previous field estimates for flow velocities of 10^{-10} - 10^{-9} m/s suggests that the obtained rates are reasonable estimates for the granitic aquifer. Since fracture zones with considerably higher water movement have been reported (up to 100 times), the effect of higher v on composition and flow has been viewed, under the assumption that obtained rate constants for redox reactions remain unchanged, thus depend only on chemical (and biological) but not on hydraulics. Fig. 5 shows the effect of variations of v under these conditions. At increased v (> 0.03 m/yr) alkalinity decreases because of the relative decrease of alkalinity flux from redox processes (Fig. 5A). This also leads to much higher amounts of SO_4^{2-} (data not shown). Hence, for faster flows, a composition differing from observed ones is predicted. On the other hand, it is obvious, that, assuming an equal increase of transformation rates, the same result is obtained as for the reference case. This, however, would imply rate constants ferric oxide and sulphate which are considerably higher than the ones reported from previous studies. Moreover, this would result in high rates of transformation with the formation of significant amounts of Fe(II) sulphide and/or siderite precipitates within the highly permeable fracture zones, which is not commonly observed (Tullborg, 1986). Therefore, we argue against the possibility of high flows (> 0.1 m/yr) controlling the major ion evolution in the deeper groundwaters. Fig.

5B shows the increase of calcite weathering (assuming calcite equilibrium) as a result of increasing v, as predicted by the model. Thus, a two-fold increase in v would give rise to a similar increase in the flux of weathered calcite. However, retardation of such high fluxes is expected by processes not considered in the model, due to diffusion and mixing with waters in the smaller fractures. This is further discussed in the section on time scales (section 5).

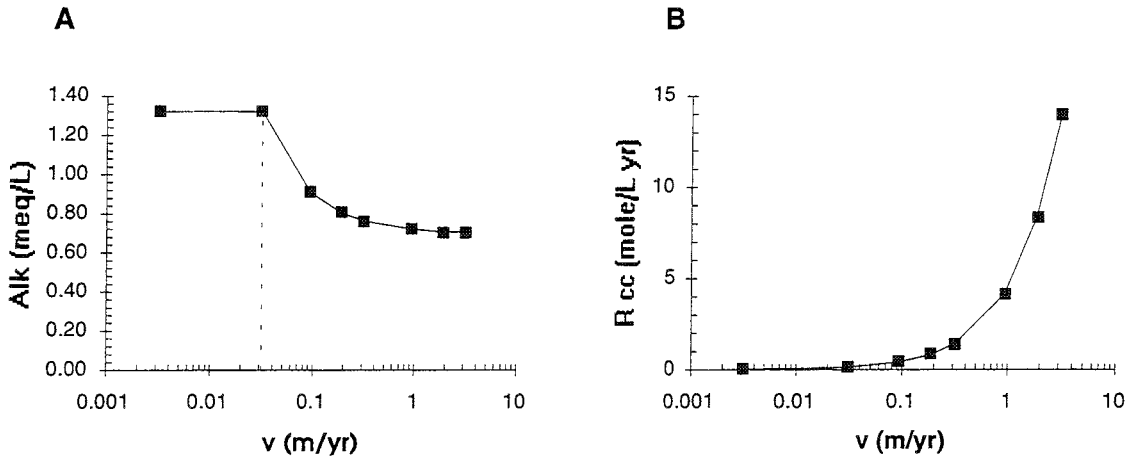

Fig. 5 Influence of flow velocity on predicted alkalinity (A) and calcite weathering rate (B). All other conditions same as for reference case, indicated by dashed line.

Mixing of different water qualities

In the modelling approach it has, so far been implicitly assumed that no mixing of waters of different origin takes place. It has been suggested (Ahlbom et al., 1992) that mixing of waters of strongly different composition does not play a major role at Klipperås, because no saline varieties have been encountered and stable data indicate meteoric origin for the water types. Nevertheless, we have tested the possibility of mixing of the shallow groundwater with a saline groundwater type, as found at Äspö. Table 7 gives the compositions of the used endmembers. The composition of mixed water (Table 7) is calculated from the average chloride concentration in the deep water, assuming chloride behaves as conservative component according to the formula: mixing ratio = (X - A)/(B - A), where X is the measured Cl-concentration in the deep groundwater, A is the Cl-concentration of endmember 1 and B is the Cl-concentration of endmember 2.

Table 7 Evaluation of possible mixing on groundwater composition. Concentrations in mM.

component	endmember 1 shallow water[a]	endmember 2 saline water[b]	deep water[c]	mixed water
Na^+	0.20	64.3	1.30	0.433
Ca^{2+}	0.20	31.3	0.60	0.313
Cl^-	0.14	138.0	0.64	0.64
SO_4^{2-}	0.20	0.624	0.021	0.202
HCO_3^-	0.10	0.667	1.86	0.102

a: average composition of spring and well data (Table 4)
b: saline water from Äspö Hard Rock Laboratory (no. KAO438A) (Banwart et al., 1992)
c: average composition of observed deep groundwater (Table 6)

The effect of such as mixing process has been taken into account by inserting the composition of the mixed water in the inflow. The results indicate a small difference with regard to the model that neglects mixing. A slight decrease in alkalinity fluxes (3 %) and calcite weathering fluxes is predicted which indicates that mixing with saline water would have no significant effect on the proton balance.

4.4 Modelling increase in acidity

4.4.1 Test case: calcite present

Based on the modelling of the present situation ("reference case") we now study the effect of acidified shallow groundwaters on the geochemistry of the deeper groundwater system. Thus, we increase the acidity of the inflow solution (by adding H_2SO_4) under the constraint of gibbsite equilibrium. Also, in these test cases the p_{CO_2} in the inflow is kept equal to the reference case (p_{CO_2} = 0.01 atm). The influence of p_{CO_2} is viewed subsequently. All other boundary condition remain unchanged. Since the kinetic processes are considered as zero-order reactions, their rates of transformation are not affected by acidifying the inflow solution. Therefore, the impact of acidity is reflected in the fast processes. In Fig. 6 the effect of acidification on pH and calcite dissolution in the deeper groundwater at steady-state conditions is illustrated. These results indicate that the composition is not significantly affected over a relatively large pH range of the inflow (pH 6-4.2) due to the high buffering capacity of the carbonate-bearing system. At lower inflow pH values the alkalinity increases due to the concurrent increase of p_{CO_2} and calcite dissolution:

$$CaCO_{3(s)} + H_2CO_3 \text{ ---> } Ca^{2+} + 2HCO_3^- \qquad (13)$$

This process is closely related to the solubility of aluminium hydroxide which strongly increases at lower pH. Thus, aluminium provides the largest pool of acidity below pH values of 4.5 which is removed via simultaneous calcite dissolution and $Al(OH)_3$ precipitation. The other potential buffering processes, such as redox processes, ion exchange, and silicate weathering yield comparatively low fluxes under these conditions.

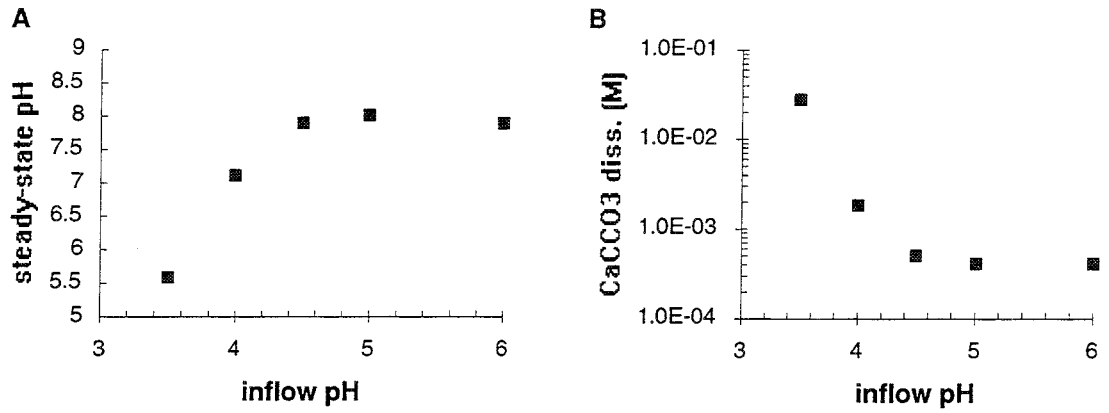

Fig. 6 Effect of increase in acidity in inflow (inflow pH) on predicted pH in lower aquifer (steady-state pH) (A) and amount of dissolved calcite in M (B).

In the next stage the effect of changing p_{CO_2} in the inflow solution is studied. This is because relatively large variations in p_{CO_2}, depending on acidity, nutrient loading, and hydraulic conditions can arise from microbial degradation of organic matter in the soil compartment The other boundary conditions are kept as in the reference case. As shown in Fig. 7 the response of the groundwater system in terms of pH and proton fluxes as a result of p_{CO_2} changes at shallow levels is significant. Thus, a strong decrease of pH and simultaneous increase of calcite weathering occurs at p_{CO_2} inflow values above about 0.01 atm. An ten times higher increase of inflow p_{CO_2} leads to about four-fold increase in calcite weathering. At lower p_{CO_2} levels than 0.005 atm, the system is not much affected by fluctuations. The results indicate that p_{CO_2} is the most sensitive chemical variable in terms of proton fluxes. On the other hand, since the model assumes a completely mixed reactor system, dilution of CO_2 gas within the aquifer with regard to soil CO_2 is not accounted for. Therefore, the model yields upper, conservative estimates for CO_2 fluxes.

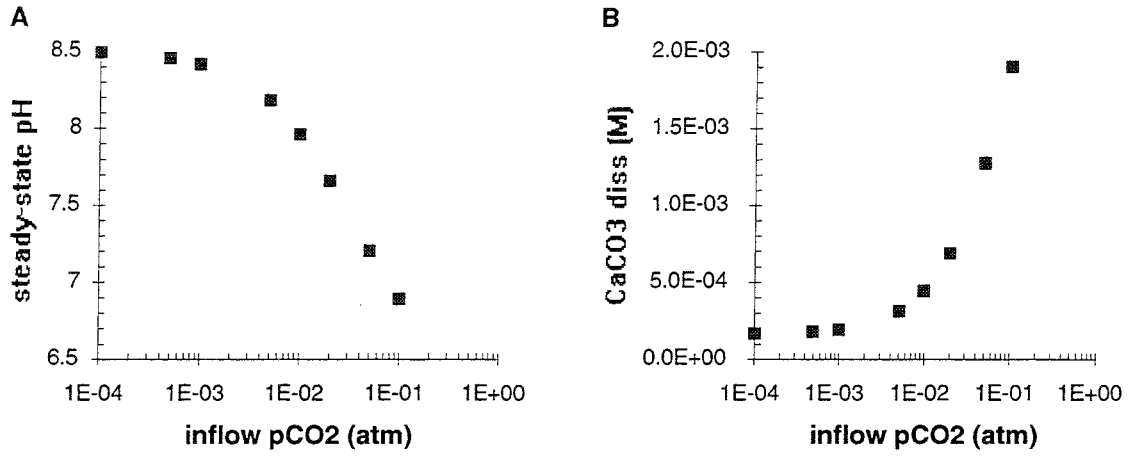

Fig. 7 Effect of the increase of p_{CO_2} in the inflow on predicted pH (A) and amount of dissolved calcite (B).

4.4.2 Test case: no calcite present

Let's consider a hypothetical future scenario where all calcite in the system has been dissolved. We again assess the effect of acidity of the inflow solution, assuming that the boundary conditions remain unchanged. Fig. 8 shows the alkalinity/acidity fluxes at steady-state with an acidified inflow solution displaying a pH of 4.5. The dominant fluxes arise from redox processes which are constrained by reaction given in Eq. 10. They are identical with the ones obtained for the reference case (Fig. 3) because the boundary conditions other than calcite equilibrium have been left unchanged. The buffering capacity of this system is largely decreased with regard to the calcite-bearing system. This is illustrated by the lowering in pH and decrease in alkalinity of the steady-state groundwater composition (Fig. 9). Nevertheless, the results indicate that relatively acidic influxes are buffered by the system. Thus, for inflow conditions higher than pH $\geq$ 4.4, the main alkalinity producing processes induce buffering with a resulting pH of about 6.5. A significant contribution to the overall buffering capacity is provided by (fast) proton exchange at clay surfaces:

$$XNa + H^+ = XH + Na^+ \qquad (14)$$

The equilibrium constant for Eq. 14 has been estimated from recent acid-base titration experiments of montmorillonite suspensions (Wanner et al., 1993; Wieland pers. comm.) to be about $K_{Na\text{-}H} = 3$. Although there are, so far, few experimental data available to support this preliminary estimate, proton exchange processes at clay surfaces appear to provide a significant acid-base buffer below pH 6 (Avena et al., 1990). Due to the uncertainties involved in the equilibrium constant, the effective CEC of the system, and the approximation

of the ion-exchange process in the present STEADYQL approach, we can, at this point only qualitatively estimate the buffering effect of proton exchange.

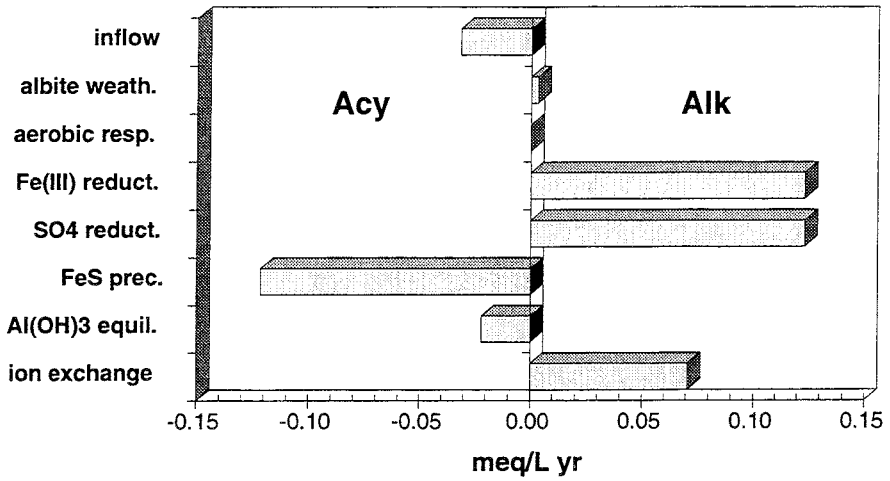

Fig. 8 Modelling groundwater system without calcite; inflow pH = 4.5. Alkalinity (+) and acidity (-) fluxes caused by chemical processes and inflow.

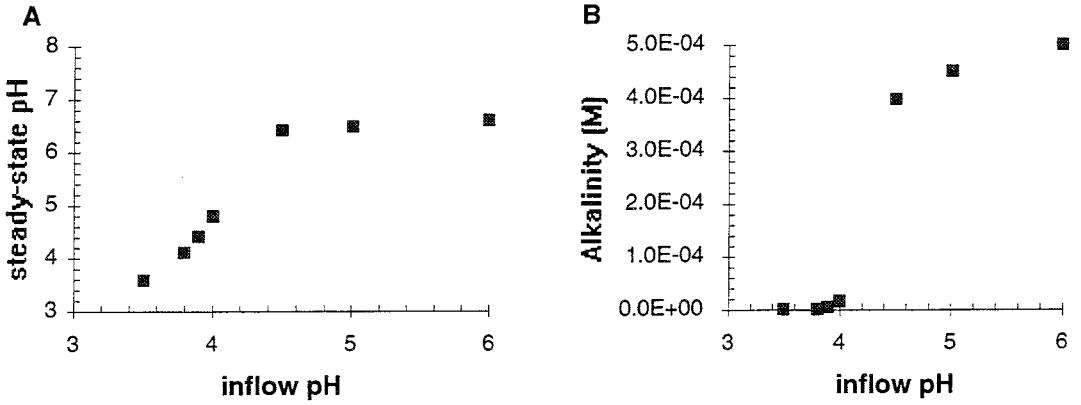

Fig. 9 Modelling system without calcite. Effect of increase in acidity in inflow on predicted pH (A) and alkalinity (B).

4.4.3 Adding soil and atmosphere

In this modelling exercise we include the soil compartment by extending our simple single-box model to a two-box model. Fig. 10 illustrates this approach schematically: Acidic atmospheric deposition (acidity input as H_2SO_4) is included as inflow into the soil compartment which reacts with the acidic influx via gibbsite equilibrium and silicate weathering. The outflow of this box is then used as inflow for the bedrock which constitutes the same model as elaborated so far. Note that the choice of different flows for each box (high in the soil and low in the bedrock) implicitly accounts for the different hydraulic regimes near the surface and at greater depths. The buffering capacity of the soil due to calcite weathering and cation exchange is assumed to be exceeded. Moreover, organic matter degradation is assumed negligible. This leaves weathering of aluminium oxide and aluminium silicate bearing minerals as main ANC process. Al is assumed to be controlled by gibbsite equilibrium, whereas silicate weathering is kinetically-controlled. Under acidic conditions, silicate weathering is enhanced compared to neutral conditions. The rate of weathering has been estimated from field data of dissolved Si concentration in the soil water (Table 6) and a flow velocity of 1m/yr to be about 3.2 10^{-11} mole Si dm^{-2} s^{-1}. The approximate composition of precipitation (rain or snow) is taken from estimations of Jacks and Knutsson (1981). Furthermore, a precipitation rate of 1000 mm/yr with an acid load of 100 meq m^{-2} yr^{-1} is converted to 0.5 mM H_2SO_4 in the inflow. This acidity influx is, according to the Rains model (Alcamo et al., 1989), a reasonable estimate for in southern Sweden strongly affected by acidification.

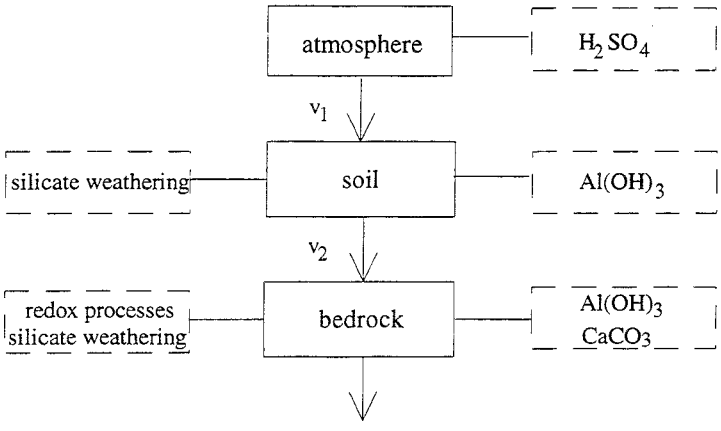

Fig. 10 Schematic view of two-box model which includes interaction of atmospheric precipitation with soil (box 1) and subsequent interaction of soil water with granitic bedrock (box 2). Each box is modelled according to site specific parameters (see text).

The results obtained for the soil box calculations indicate a solution composition similar to the one observed for the most acidic soil water (Tallebo spring, Table 6). Thus, the obtained pH = 4.2, Al = 0.29 mM, and Si = 0.10 mM agree well with observed values. The obtained SO_4^{2-} concentration (0.57 mM) is considerably higher than observed levels which could arise from the fact that a part of the acidity arises from the nitrogen influx (Rohde and Granat, 1984) and/or from sorption of SO_4^{2-} at low pH. Nevertheless, the overall results suggest, that the proposed, very simple model predicts composition of poorly buffered granitic soils reasonably well. The proton fluxes within the soil are summarized in Fig. 11.

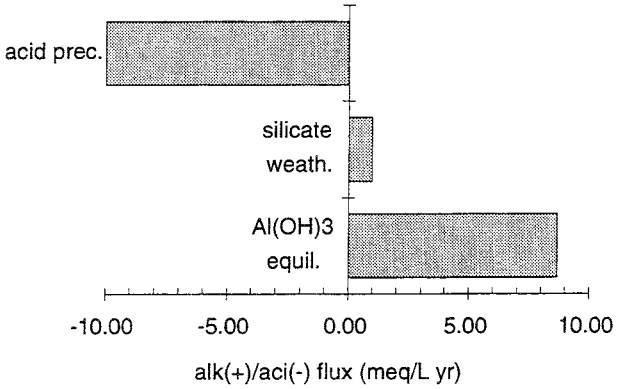

Fig. 11 Alkalinity/acidity fluxes in the modelled soil compartment. For boundary conditions see text.

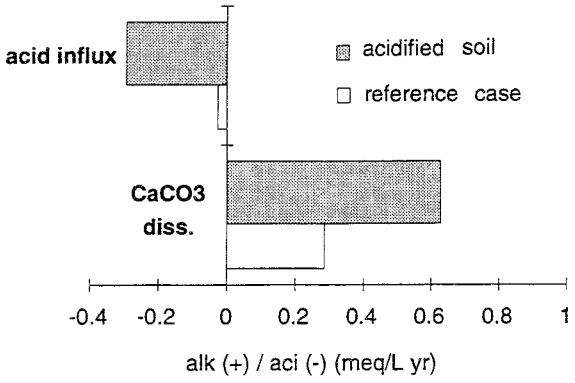

Fig. 12 Alkalinity/acidity fluxes predicted for the deeper aquifer as a result of increased soil acidification (shaded area). Predicted fluxes for actual situation also shown (unshaded area).

In the next step the influence of the acidified soil on the deeper groundwater is modelled. The results show that the increased acidity influx leads to a higher flux of dissolved calcite with regard to the reference case. Fig. 12 illustrates there is a predicted ten-fold increase of acidity

influx for the acidified soil compared to the actual situation whereas the resulting alkalinity flux increases by a factor of 2.2. This indicates that under severe conditions of soil acidification the granitic aquifer buffers the acidity load such that calcite weathering increases relatively moderately.

4.5 Summary of buffering mechanisms

The main process buffering acidity is calcite weathering which provides the dominant source of alkalinity. Thus, the deeper groundwater system shows inert behavior towards a large range of acidic influx. Processes involving iron, sulphur, and organic carbon cycling strongly affect alkalinity fluxes and lead to enhanced calcite weathering. Acidity fluxes due to aluminium mobilization are strongly increased above a threshold value of acidic input. This, in turn, leads to a strong increase of calcite weathering. A further important factor is p_{CO_2} at shallow levels which may strongly depend on microbially-induced degradation of organic matter in the soil. Thus, high levels of p_{CO_2} in the inflow also result in increased calcite weathering. The effect of a weathered, acidified soil on the proton fluxes of the deeper aquifer is not very large. Thus, an enhancement of the weathered calcite flux by a factor of about two is expected once the shows no buffering capacity other than through Al and Si weathering.

In a system where all calcite has dissolved, the acid neutralizing capacity (ANC) is largely decreased. Acidity is neutralized to a certain extent by redox processes and proton exchange processes. Once the acidity flux, which is dominated by aluminium equilibrium reactions exceeds the alkalinity fluxes provided by the former processes, the ANC of groundwater system becomes very low. It would be then mainly provided by silicate weathering whose contribution to alkalinity is much lower compared to the other processes invoked.

From these findings the effect of acidification on a groundwater fracture zone (Klipperås) can be schematically presented by Fig. 13 which qualitatively shows the alkalinity of the deep groundwater solution as a function of time. At stage 1 the effect of acidification (present situation) is insignificant since there is still sufficient buffering capacity in soil (low Al mobility). Once Al is mobilized because the buffering capacity of the overlying soil has largely diminished or if p_{CO_2} strongly increases at shallow levels, calcite weathering and alkalinity will increase until a new constant acidity or CO_2 influx is reached (stage 2) After exhaustion of the carbonate buffer, the buffering capacity will be reduced and controlled by redox processes and proton-clay surface interaction which still provide a notable buffering mechanism (stage 3). At stage 4, once the acidic influx exceeds the alkalinity fluxes, the

system will react much more sensitively to changes in acidity fluxes, the principal remaining process contributing to the ANC being silicate weathering.

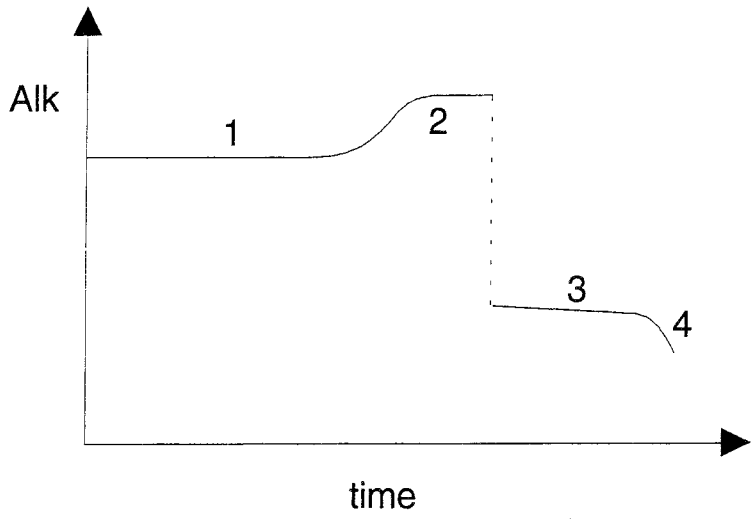

Fig. 13 Possible qualitative evolution of alkalinity in granitic groundwater as a result of acidification, as predicted by the model. For explanations see text.

5 Time scales

5.1 Concept

The model we have presented so far has shown to give consistent results for a granitic aquifer. In this section we discuss the implications of the modelling results in the light of HLW repository safety. The main factors which contribute to the decrease of the buffering capacity in the deeper aquifer will be highlighted. This particularly concerns factors which lead to enhanced calcite weathering. The main emphasis is to focus on time scales of calcite depletion (stages 1 and 2 in Fig. 13). The evolution of the buffering capacity of the aquifer depleted with carbonates (stages 3 and 4) which is difficult to estimate quantitatively due to the lack of available data, will not be considered.

5.2 Major factors

5.2.1 Acidification scenarios

The time evolution of acid load depends on climatic scenarios and the reduction measures put into place (Nebot and Bruno, 1991). Here we will limit the discussion to the case where control measures are low in order to be conservative in the assessment of time scales. Using predictions of the Rains model (Alcamo et al., 1989), for sulphur and nitrogen deposition rates in southern Sweden, conservative estimates for the next decades yield 1-2 g S m^{-2} yr^{-1} and 1 g N m^{-2} yr^{-1}. These values are considered to be beyond critical loads for sensitive ecosystems. The deposition rates are converted to acidity fluxes by attributing half of S to sulphuric acid (the other half to aerosol particles) and all N to nitric acid. This amounts to an acidity load of 103 - 134 meq m^{-2} yr^{-1} which is about the same as assumed in our previous calculations on soil acidification (section 4.4.3). Acid precipitation is expected to decrease beyond about the year 2300 because of depletion of fossil fuels. After this time, since the residence times of SO_2 and NO_x are short, rapid decrease of the acid load will occur.

In the subsequent estimations we assume that by the year 2000 the soil will be acidified to conditions outlined in section 4.4.3, which include calcite depletion, depletion of the organic-rich layer, and excess of the buffer capacity of the cation exchange range. This assumption of rapid degradation of the soil may be over conservative for the forested Klipperås area with a thick soil layer but may well apply to other granitic areas in Sweden which often display very thin podsolic layers. After the year 2300 a ten-fold decrease of the acidic influx to 10 meq m^{-2} yr^{-1} is assumed.

5.2.2 Hydraulic conditions

The modelling results suggest an average flow velocity for the Klipperås aquifer of 10^{-10} - 10^{-9} m/s (section 4.3.3). For a block of 500 m this would correspond to a residence time for the waters of 160'000 to 16'000 years. In SKB 91 (1992) the hydrologic pathways of a highly fractured aquifer (Finnsjön) are summarized as travel times from the repository to the ground surface (Fig. 14). The major fraction of water is predicted to have travel times of 10'000 years which is somewhat shorter than predicted for the Klipperås area. A minor fraction of water, however, moves significantly faster with a peak of a factor of 100 with regard to the major fraction (Fig. 14). This reflects flow through highly permeable fractures.

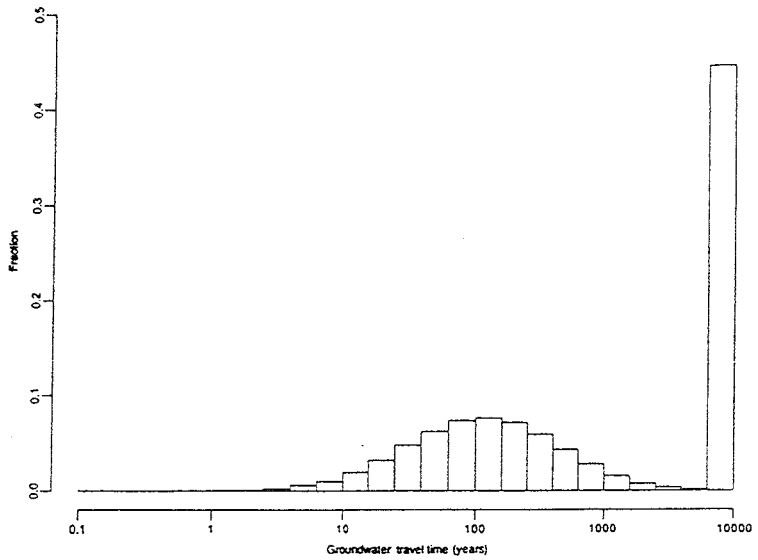

Fig. 14 Histogram of travel time for water from repository to surface estimated for Finnsjön area. Taken from SKB-91.

The impact of the fast moving water fraction on the buffering capacity of the aquifer towards acidic influx is difficult to predict with our simple steady state model. As discussed in section 4.3.3 if fast flow were controlling major chemistry an increase of alkalinity fluxes and redox transformation rates, according to the model, of almost two order of magnitude would result. On the other hand dilution will occur via dispersion and mixing with waters of slower flow velocities (Appelo and Postma, 1993). Furthermore, it is likely that the p_{CO_2} is decreased due to the relative decrease of organic matter transformation rates and diffusion-limitation of the high CO_2 flux from the soil. All these factors would retard high calcite weathering fluxes and contribute to a more homogeneous distribution of acidity and alkalinity fronts within the aquifer. The relevance for these retardation mechanisms is supported by the usually relatively homogeneous chemistry observed in most granitic aquifers.

5.2.3 Amount and distribution of calcite

Estimation of the calcite concentrations in the aquifer is critical for assessing time scales. This is a difficult task due to the scarcity of data. Fortunately, in the case of the Klipperås study site there is some information concerning calcite-coatings in fractures (Tullborg, 1986; Tullborg, pers. communication). Thus, according to Tullborg, in the near-surface region (0-40/50 m) calcite-fillings are nearly absent, whereas they are present in most fractures (60-80 %) below 100 m and cover 15 to 30 % of the surfaces. Thin section analysis suggests coating thicknesses of about 0.5 mm. In the fracture zones between 50 and 100 m the frequency of calcite-bearing fractures strongly varies. In some high conductivity fractures calcite has found to be absent down to more than 100 m. These observations indicate that calcite weathering is in fact an active process and support findings from our model. Furthermore, it reveals the

front character of calcite decrease which is not accounted for in the single-box model. A refinement to a multi-box model would require an extended set of depth-depended geochemical data. However, results from the presented single-box model are useful, since they yield conservative estimates of weathering fluxes compared to more refined models which account for propagation of fronts.

The amount of calcite in the fracture zones of the deeper aquifer (below 100 m depth) can be roughly estimated from above information by assuming that fracture-coatings are the only source of calcite. Taking radar measurement data by Andersson et al. (1989) who estimated flow porosities of about $2 \cdot 10^{-4}$ and wetted surface areas 0.7 - 4 m^2 per m^3 of rock and taking an average of 20 % of surface coverage for calcite particles with a thickness of 0.5 mm then the percentage of calcite in the rock is 0.007 - 0.04 %. Taking a density of 2.65 kg/dm^3, this corresponds to 9.3 to 53 mole calcite per L of porewater. For fracture zones of high hydraulic conductivity flow porosities of around 0.01 are reasonable (Andersson et al., 1993). Assuming that the wetted surface area increase proportionally to the increase in porosity, the proportion of calcite, at the same surface coverage, should also increase proportionally to 0.035 - 0.2 %. Thus, the same calculation as above yields very similar calcite amounts (9.2 - 52 mole L^{-1}). Note that the estimated calcite amount corresponds to the pool of calcite-bearing fractures. On the other hand, small fractures (~ 1 mm) filled with fracture minerals (mainly calcite, epidote, chlorite, and/or ferric oxide) indicate an additional calcite-pool (Banwart et al., 1992). Therefore, the suggested values corresponds to conservative estimates.

The observations above further suggest that calcite in high-conductivity fractures has been depleted to greater depths compared to the main bulk of fractures. This is qualitatively in agreement with model calculations which predict higher weathering rate at higher flow However, the weathering rate does not appear to increase linearly with flow but increases much more slowly. Assuming a simple steady weathering rate over a depth of 100 meters and the same amount calcite per volume of water (see above), the increase of calcite weathering would be about a factor of two for a fracture of 50 to 100 times higher hydraulic conductivity. This suggests that the factors outlined in above section, in fact, do retard high weathering fluxes in high conductivity zones.

5.2.4 Partial pressure of CO_2

As model calculations have revealed (sections 4.3.3 and 4.4.1) p_{CO_2} is the most critical chemical variable influencing acidity/alkalinity fluxes in the presence of calcite. As has been pointed out, the model assumes a closed system with regard to CO_2 exchange. Moreover, since an inherent model assumption is complete mixing in the reactor box, the high CO_2

influx from the soil is assumed to be mixed throughout the deeper aquifer. This is in fact a conservative assumption because losses of CO_2 pressure in via diffusional processes are expected to occur. Therefore, the predicted p_{CO_2} and resulting calcite weathering rates represent upper estimates. Fig. 15 shows the relationship between p_{CO_2} in the deeper aquifer and calcite weathering rate. The range of expected p_{CO_2} from model calculations (section 4.3.3) is also shown.

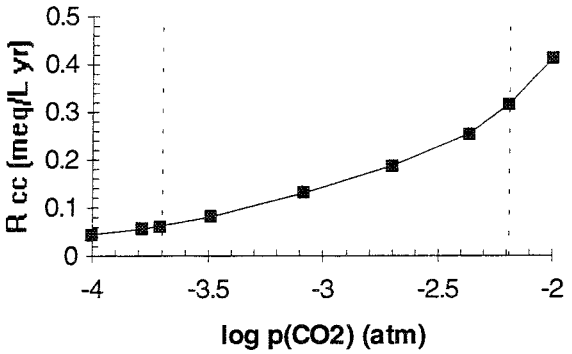

Fig. 15 Relationship between partial pressure of CO_2 vs. calcite weathering rate in the lower aquifer. Dashed lines illustrate range of expected p_{CO_2}.

Besides influx from the top layer, p_{CO_2} is affected by organic matter degradation in the deeper parts. Enhanced soil weathering as a result of acidification is expected to decrease amount of degradable organic matter. This, in turn, may decrease microbiological activity in the lower aquifer which lead to lower p_{CO_2}. Thus, acidification may trigger a negative feed back mechanism for CO_2 evolution. This would further limit the amount of weathered calcite flux.

5.3 Synthesis

From discussion of the range of the major factors which influence calcite weathering we now attempt to estimate time scales of calcite depletion. A step-wise procedure will be followed: First time scales of depletion obtained directly from the single-box model taking realistic ranges of p_{CO_2} and calcite concentrations will be deduced. Second, the influence of fast flow and front propagation on time scales will be discussed. Third, the time evolution of acidification will be taken into account. Finally, two scenarios will be proposed.

The impact of the uncertainty range of p_{CO_2} and calcite amount in the lower granitic aquifer on time scales of calcite depletion under conditions of an upper range of bulk flow velocity (10^{-9} m/s) are presented in matrix form in Table 8. The range of uncertainty for p_{CO_2} is about

5 10^{-4} - 10^{-2} atm and for calcite 0.007 - 0.04 weight % or 9.3 - 53 mole per liter of water. Taking calcite weathering rates illustrated in Fig. 15 time scales of calcite depletion range from 22 500 - 658 300 years.

Table 8 Time scales of calcite depletion in the granitic aquifer at 500 m depth calculated from the single-box model for a flow velocity of 10^{-9} m/s at different p_{CO_2} (atm) and weight % calcite (% cc) in the aquifer.

% cc \ p_{CO_2}	10^{-4}	5 10^{-4}	10^{-3}	5 10^{-3}	10^{-2}
0.007	209 009	115 202	66 235	49 261	22 509
0.01	298 585	164 574	94 621	70 373	32 155
0.02	597 169	329 148	189 243	140 747	64 311
0.03	895 754	493 722	283 864	211 120	96 466
0.04	1 194 338	658 297	378 486	281 494	128 621

Furthermore, time scales are affected by the transport mechanisms occurring in the aquifer which mainly include fast flow in high conductivity fractures and front propagation of the weathered zone. The former will enhance whereas the latter will retard calcite weathering. From mineralogical observation it is suggested that the zone of calcite depletion is about twice as deep for high conductivity fractures compared to the main fracture zone. On the other hand, calcite-filled micro fractures are present which will contribute to retardation. From these observations and the factors discussed in section 5.2.2 we assume that fast flow increases the overall rate of depletion of calcite by a factor of between 2 and 5. The transient behaviour of calcite depletion is not accounted for in the proposed steady-state model. However, this behaviour can be roughly approximated by assuming various boxes of certain thickness. From mineralogical observations it can be inferred that the upper 0- 40/50 m are strongly impoverished in calcite whereas the zones below 100 m contain significant concentrations of calcite precipitates. The intermediate zone indicates partly decreased amounts of carbonate. On the basis of this information let us assume that a box of 50- 100 m thickness can be roughly approximated by steady-state conditions and assign five boxes for the interval of 0-500 m depth. Under conditions of no change in flow properties in time and space, depletion of calcite at 500 m depth would then be retarded by at least a factor of 4-5 depending on how long the top box is expected to be completely depleted in calcite.

The influence of acid deposition will, under severe conditions, lead to a strong decrease of the soil buffering capacity and depletion of the organic-rich soil layer in the next 300 years, as outlined in section 5.2.1. This is predicted to enhance calcite weathering in the lower aquifer by a factor of 2.2 to 3.0. An assumed subsequent decreased acidity input of a factor of ten

would strongly decrease calcite weathering, especially under the condition of no organic layer in the soil which decreases p_{CO_2} in the soil. This would lead to a predicted decrease of calcite weathering by a factor of about two with regard to the reference case. In the case, that soil conditions similar to the present situation reasons will reestablish, the weathering of calcite is expected to be only slightly lower than predicted at present.

Two different scenarios are proposed to estimate time scales of calcite depletion and decreased buffering in the granitic aquifer down to a depth of 500 m. In scenario 1 a very conservative case is envisioned:

- influence of high-conductivity fractures increases overall weathering rate by factor of five with regard to reference case
- minimum amount of estimated calcite: 0.007 % (9 mole per L water)
- acid precipitation load: 134 meq m^{-2} yr^{-1} for 300 years, then soil conditions according to present situation
- steady-state condition for entire depth of 500 m (one-box model).

In scenario 2 a more realistic case with regard to discussed is assumed:

- influence of high-conductivity fractures increases overall weathering rate by factor of two
- average amount of estimated calcite: 0.02 % (26.5 mole per L of water)
- acid precipitation load: 103 meq m^{-2} yr^{-1} for 300 years, then soil conditions according to present situation
- steady-state conditions for compartments of 100 m (five-box model).

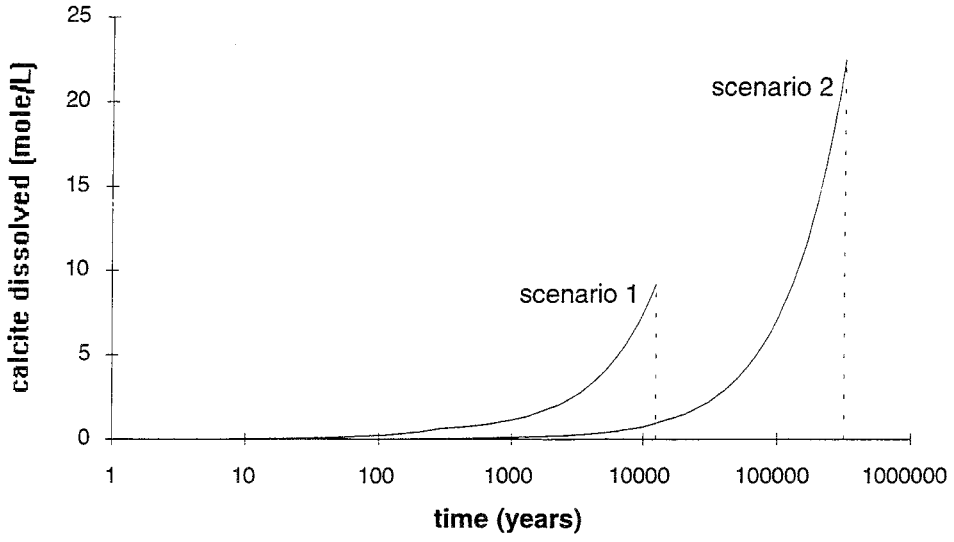

Fig. 16 Time evolution of calcite decrease in the aquifer according to two different scenarios (see text).

The outcome of both scenarios is illustrated in Fig. 16. Thus, according to scenario 1 calcite depletion will occur after 12 400 years whereas in scenario a time scale of 370 000 years is predicted.

5.4 Further uncertainties

The range of uncertainty of the major parameters (hydrology, p_{CO_2}, calcite content, acidity scenario) affecting the carbonate buffer has been discussed in above sections. Here, we briefly discuss the impact of other factors.

Al-mobility: Under acidic conditions Al-mobility dominates the acidity flux. In the model we have assumed $Al(OH)_3$ equilibrium which in fact is a conservative assumption since, via ion exchange with clay surfaces and humic material, observed dissolved Al concentrations are considerably lower at pH < 4.5 (Appelo and Postma, 1993; Mulder and Stein, 1994).

Temperature: The model takes into account thermodynamic constants valid for 25 °C. This is a somewhat an intermediate temperature for the granitic aquifer which increases from about 10 °C at the top to about 50-60 °C at 500 m depth. The increase of temperature with depth contributes to retardation of calcite weathering due to the lower solubility of calcite at higher temperature.

6 Summary and conclusions

We have presented a simple box steady-state model based on the STEADYQL algorithm which describes the effect of acidification on the geochemical behaviour of a granitic aquifer. This model is applied to the Klipperås study site in order to test its validity and to evaluate proton fluxes in granitic fracture zones. The boundary conditions are assessed on the basis of the available hydrogeological and geochemical information on the Klipperås site and from recent work performed in the Äspö Hard Rock Laboratory. These include (1) inflow of slightly acidic shallow groundwater, (2) constant downward flow through a fracture zone of relatively high permeability, (3) interaction of moving groundwater with fracture-filling minerals, (4) biologically-mediated degradation of organic matter.

The modelling results show that the derived composition of the deep groundwater is in remarkable agreement with the observed levels of major components. This indicates that the model offers an adequate description of the geochemical evolution of the aquifer. The

dominant acid neutralizing process is calcite weathering. Microbially-mediated degradation of organic matter significantly affects the proton balance and their interplay with the carbonate equilibria determines alkalinity and p_{CO_2}. Ion exchange at clay surfaces notably increases calcite weathering via Na-Ca exchange. Silicate weathering is found contribute only slightly to alkalinity production. The derived rate constants for Fe(III) oxide under the constraint of iron sulphide precipitation and the imposed flow velocity are consistent with reported experimental data. A sensitivity analysis of the inflow variables indicates that the modelling results are not significantly affected by uncertainties associated major ion concentration. However, the model is found to be very sensitive with regard to soil p_{CO_2}. Furthermore, the model results are not significantly affected when mixing of different water qualities is included.

The model is further used to predict the effect of acidification on deep groundwater and three different test cases are constructed. In the first, the impact of increased acid load via addition of sulphuric acid to the shallow groundwater is evaluated. The results indicate that the granitic aquifer is an effective buffer up to relatively high levels acidic influx. Beyond this level, the flux of dissolved calcite strongly increases and resulting pH decreases mainly as a result of increased aluminium mobility in the inflow. In the second test case the effect of CO_2 partial pressure in the inflow is evaluated. The results are analog to the first case, in that they indicate inert behaviour of the system over a large range of p_{CO_2} conditions and increase in calcite weathering and alkalinity beyond a threshold of $p_{CO_2} \approx 5 \cdot 10^{-3}$ atm. In the third case a potential future scenario is envisioned in which all calcite has been removed by continuos weathering. The buffering capacity which is now dominated by anaerobic respiration processes is largely reduced. Also, the results suggest that proton exchange reactions at clay surfaces provides a significant fraction to the acid neutralizing capacity. At high ongoing influxes of acidity the alkalinity fluxes are neutralized and the system reacts strongly to small fluctuations in the proton balance.

The model is extended to a two-box model by including a simplified soil compartment and the actual acidic load from the atmosphere. The results indicate that the model shows good agreement with the composition of strongly acidified soil waters found in the area. The increase in alkalinity fluxes in the deeper aquifer as a result of increased soil acidity is predicted to be a factor between 2 - 3 with regard to the actual fluxes.

An estimation of time scales of aquifer acidification under the focus of calcite depletion has been assessed by taking into account mineralogical data on calcite distribution in fracture zones and radar data on flow porosity and wetted surface area. Further, the influence of the fast moving water fraction on calcite weathering is considered. The effect of increased acidity

within the next 300 years is also included in two acidification scenarios. From the two scenarios a time scale of 12 400 to 370 000 years is estimated for calcite depletion down to 500 m depth. It is suggested that this presents a conservative time range, since estimates are based on assumed steady-state conditions over large depths (100 - 500 m). Furthermore, model assumptions with regard to Al-mobility and temperature also point to the conservative character of the proposed estimates.

7 Acknowledgments

This work greatly benefited from discussions with Steven Banwart (KTH) , Eva-Lena Tullborg (Terralogica), Bill Wallin (Geokema), Peter Wikberg (SKB), and Gerhard Furrer (ETH Zürich).

8 References

Ahlbom K., Andersson J.-E., Andersson P., Ittner T., Ljunggren C., Tirén S. (1992) Klipperås study site. Scope of activities and main results. SKB TR 92-22.

Alcamo J., Bartnicki J., Schöpp W. (1989) Long-range transport of sulfur and nitrogen compounds in Europe's atmosphere. In The Rains Model of Acidification (eds. Hordijk L., Shaw R., Alcamo J.) Kluwer Academic Publishers, Dordrecht, pp. 115-178.

Andersson P., Andersson P., Gustafsson E., Olsson O. (1989) Investigation of flow distribution in a fracture zone at the Stripa mine, using the radar method, results and interpretation. SKB TR 89-33.

Andersson P., Nordqvist R., Persson T., Eriksson C.-O., Gustafsson E., Ittner T. (1993) Dipole tracer experiment in a low-angle fracture zone at Finnsjön- results and interpretation. The Fracture Zone Project-Phase 3. SKB TR 93-26.

Appelo A. and Postma D. (1993) Geochemistry, groundwater, and pollution. Bakema, Rotterdam.

Avena M.J., Cabrol R., De Pauli C.P. (1990) Study of some physicochemical properties of pillared montmorillonites: Acid-base potentiometric titrations and electrophoretic measurements. Clays Clay Min. 38, 356-362.

Banwart S., Gustafsson E., Laaksoharju M., Nilsson A.-C. Tullborg E.-L., Wallin B. (1994) Redox processes in a granitic coastal aquifer. Water Resour. Res. (in press).

Banwart S., Laaksoharju M., Nilsson A.-C. Tullborg E.-L., Wallin B. (1992) The large scale redox experiment. Initial characterization of the fracture zone. Äspö Hard Rock Laboratory SKB Progress Report 25-92-04.

Berner R.A. (1981) A new geochemical classification of sedimentary environments. J. Sediment. Petrol. 51, 359-365.

Brömssen von U. (1989) Acidification trends in Swedish groundwaters. Review of time series 1950-85. National Swedish Environmental Protection Board Report 3547.

Canfield D.E. (1989) Reactive iron in marine sediments. Geochim. Cosmochim. Acta 53, 619-632.

Cosby B.J., Hornberger G.M., Rastettler E.B., Galloway J.N., Wright R.F. (1986) Estimating catchment water quality response to acid deposition using mathematical models of soil ion exchange processes. Geoderma 38, 77-95.

Davis G.F., Whipple W.J., Gherini S.A., Chen C.W., Goldstein R.A., Johannes A.H., Chan P.W.H., Munson R.K. (1987) Big Moose Basin: simulation of response to acidic deposition. Biogeochem. 3, 141-161.

Drever J.I., Zobrist J. (1992) Chemical weathering of silicate rocks as a function of elevation in the southern Swiss Alps. Geochim. Cosmochim. Acta 56, 3209-3216.

Driscoll C.T., Likens G.E. (1982) Hydrogen ion budget of an aggrading forested watershed. Tellus 34, 283-292.

Furrer G. (1991) Theorie der Bodenversauerung: das Zusammenspiel verschiedener Ursachen. Bodenkundliche Gesellschaft der Schweiz, BGS - Bulletin 15, 1-14.

Furrer G., Westall J., Sollins P. (1989) The study of soil chemistry through quasi-steady-state models: I. Mathematical definition of model. Geochim. Cosmochim. Acta 53, 595-601.

Furrer G., Westall J., Sollins P. (1990) The study of soil chemistry through quasi-steady-state models: II. Acidity of soil solutions. Geochim. Cosmochim. Acta 54, 2363-2374.

Gherini S.A., Mok L., Hudson J.M., Davis G.F., Chen C.W., Goldstein R.A. (1985) The ILWAS model: formulation and application. Water Air soil Pollut. 26, 425-460.

Gentzschein B. (1986) Hydrogeological investigations at the Klipperås study site. SKB TR 86-08.

Hordijk L., Shaw R., Alcamo J. (1989) Background to acidification in Europe. In The Rains Model of Acidification (eds. Hordijk L., Shaw R., Alcamo J.) Kluwer Academic Publishers, Dordrecht, pp. 31-61.

Jacks G., Knutsson G. (1981) Susceptibility of groundwaters to acidification in different parts of Sweden. Kol, Hälsa, Miljö, Report 11.

Knauss K., Wolery T.J. (1986) Dependence of albite dissolution kinetics on pH and time at 25°C and 70°C. Geochim. Cosmochim. Acta 50, 2481-2497.

Knutsson G. (1970) Om grundvatten och vattenförsörjning. Avd för Geol., Tekniske fakulteten, Lunds Universitet.

Knutsson G. (1971) Ground water in till soils. GFF 93.

LaKind J., Stone A. (1988) Reductive dissolution of goethite by phenolic reductants. Geochim. Cosmochim. Acta 53, 961-972.

Laurent S. (1986) Analysis of groundwater from deep boreholes in Klipperås. SKB TR 86-17.

Lindbom B., Lundblad K., and Winberg A. (1988) Groundwater flow modelling at the Klipperås site: Regional and subregional scale. SKB Progress Report AR 88-12.

Lovley D.R. (1987) Organic matter mineralization with reduction of ferric iron: a review. Geomicrobiology J. 5, 375-400.

Mulder J. and Stein A. (1994) The solubility of aluminum in acidic forest soils: Long-term changes due to acid deposition. Geochim. Cosmochim. Acta 58, 85-94.

Nebot J., Bruno J. (1991) The implications of soil acidification on a future HLW repository. Part I: The effects of increased weathering, erosion, and deforestation. SKB TR 91-45.

Nikolaidis N.P., Rajaram H., Schnoor J.L., Georgakos K.P. (1988) A generalized soft water acidification model. Water Resources Res. 24, 1983-1996.

Olkiewicz A., Stejskal V. (1986) Geological and tectonic description of the Klipperås study site. SKB TR 86-06.

Rohde H., Granat L. (1984) An evaluation of sulfate in European precipitation 1955-1982. Atmosph. Environm. 18, 2637-2639.

Schnoor J.L., Stumm W. (1985) Acidification of aquatic and terrestrial systems. In Chemical Processes in Lakes (ed. W. Stumm), Wiley & Sons, pp. 311-338.

Schnoor J.L., Palmer W.D., Jr., Glass G.E. (1984) Modelling impacts of acid precipitation for northeastern Minnesota. In Modelling of Total Acid Precipitation Impacts (ed. J.L. Schnoor); Acid Precipitation Ser 9, pp. 155-173. Butterworth.

Sehlstedt S., Stenberg L. (1986) Geophysical investigations at the Klipperås study site. SKB TR 86-07.

SKB 91. Final disposal of spent fuel. Importance of the bedrock for safety (1992). Swedish Nuclear Fuel Supply Co/Division KBS, Stockholm.

Smellie J., Larsson N.-A, Wikberg P., Carlsson L. (1985) Hydrochemical investigation in crystalline bedrock in relation to existing hydraulic conditions: Experience from the SKB test-sites in Sweden. SKB TR 85-11.

Smellie J., Larsson N.-A., Wikberg P., Puigdomenech I., Tullborg E.-L. (1987) Hydrochemical investigation in crystalline bedrock in relation to existing hydraulic conditions: Klipperås test-site, Småland, Southern Sweden. SKB TR 87-21.

Sposito G. (1983) Surface chemistry of soils. Oxford University Press, New York.

Sulzberger B., Suter D., Siffert C., Banwart S., Stumm (1989) Dissolution of Fe(III) (hydr)oxides in natural waters; laboratory assessment on the kinetics controlled by surface coordination. Marine Chem. 28, 127-144.

Tullborg E.-L. (1986) Fissure fillings from the Klipperås Study Site. SKB TR 86-10.

Ulrich B. (1981) Eine ökosystemare Hypothese über die Ursache des Tannensterbens. Forstwiss. Centralbl. 100, 228-239.

Ulrich B., Mayer R., Khanna P.K. (1980) Chemical changes due acid precipitation in a loess-derived soil in Central Europe, Soil Sci. 130, 193-215.

Velbel M.A. (1985) Geochemical mass balances and weathering rates in forested watersheds of the southern Blue Ridge. Amer. J. Sci. 285, 904-930.

Wanner H. (1986) Modelling interaction of deep groundwaters with bentonite and radionuclide speciation. Nagra NTB 86-21, Baden, Switzerland.

Wanner H., Albinsson Y., Karnland O., Wieland E., Wersin P., Charlet L. (1993) The bentonite chemical model: Phases II/III Surface characteristics of montmorillonite. SKB Progress Report (in press).

Wersin P., Höhener P., Giovanoli R., Stumm W. (1991) Early diagenetic influences on iron transformations in a freshwater lake sediment. Chem. Geol. 90, 233-252.

Westall J.C. (1986). MICROQL. A chemical equilibrium program in BASIC. Version 2 for PCs. Report 86-02, Dept. of Chemistry, Oregon State University, Corvallis, OR, 44p.

Wikberg P., Axelsen K., Fredlund F. (1987) Deep groundwater chemistry. SKB TR 87-07.

Winberg A., Gentschein B. (1987) Model calculations of the groundwater regime at Klipperås - Approach on a regional and subregional scale SGAB IRAO 87415 (in Swedish).

Zobrist J., Sigg L., Schnoor J.L., Stumm W. (1987) Buffering mechanisms in acidified alpine lakes. In Reversibility of Acidification (ed. H. Barth), CEC Brussels, Elsevier Applied Science, Barking UK, pp. 95-103.

List of SKB reports

Annual Reports

1977-78
TR 121
KBS Technical Reports 1 – 120
Summaries
Stockholm, May 1979

1979
TR 79-28
The KBS Annual Report 1979
KBS Technical Reports 79-01 – 79-27
Summaries
Stockholm, March 1980

1980
TR 80-26
The KBS Annual Report 1980
KBS Technical Reports 80-01 – 80-25
Summaries
Stockholm, March 1981

1981
TR 81-17
The KBS Annual Report 1981
KBS Technical Reports 81-01 – 81-16
Summaries
Stockholm, April 1982

1982
TR 82-28
The KBS Annual Report 1982
KBS Technical Reports 82-01 – 82-27
Summaries
Stockholm, July 1983

1983
TR 83-77
The KBS Annual Report 1983
KBS Technical Reports 83-01 – 83-76
Summaries
Stockholm, June 1984

1984
TR 85-01
Annual Research and Development Report 1984
Including Summaries of Technical Reports Issued during 1984. (Technical Reports 84-01 – 84-19)
Stockholm, June 1985

1985
TR 85-20
Annual Research and Development Report 1985
Including Summaries of Technical Reports Issued during 1985. (Technical Reports 85-01 – 85-19)
Stockholm, May 1986

1986
TR 86-31
SKB Annual Report 1986
Including Summaries of Technical Reports Issued during 1986
Stockholm, May 1987

1987
TR 87-33
SKB Annual Report 1987
Including Summaries of Technical Reports Issued during 1987
Stockholm, May 1988

1988
TR 88-32
SKB Annual Report 1988
Including Summaries of Technical Reports Issued during 1988
Stockholm, May 1989

1989
TR 89-40
SKB Annual Report 1989
Including Summaries of Technical Reports Issued during 1989
Stockholm, May 1990

1990
TR 90-46
SKB Annual Report 1990
Including Summaries of Technical Reports Issued during 1990
Stockholm, May 1991

1991
TR 91-64
SKB Annual Report 1991
Including Summaries of Technical Reports Issued during 1991
Stockholm, April 1992

1992
TR 92-46
SKB Annual Report 1992
Including Summaries of Technical Reports Issued during 1992
Stockholm, May 1993

1993
TR 93-34
SKB Annual Report 1993
Including Summaries of Technical Reports Issued during 1993
Stockholm, May 1994

Technical Reports
List of SKB Technical Reports 1994

TR 94-01
Anaerobic oxidation of carbon steel in granitic groundwaters: A review of the relevant literature
N Platts, D J Blackwood, C C Naish
AEA Technology, UK
February 1994

TR 94-02
Time evolution of dissolved oxygen and redox conditions in a HLW repository
Paul Wersin, Kastriot Spahiu, Jordi Bruno
MBT Technología Ambiental, Cerdanyola, Spain
February 1994

TR 94-03
Reassessment of seismic reflection data from the Finnsjön study site and prospectives for future surveys
Calin Cosma[1], Christopher Juhlin[2], Olle Olsson[3]
[1] Vibrometric Oy, Helsinki, Finland
[2] Section for Solid Earth Physics, Department of Geophysics, Uppsala University, Sweden
[3] Conterra AB, Uppsala, Sweden
February 1994

TR 94-04
Final report of the AECL/SKB Cigar Lake Analog Study
Jan Cramer (ed.)[1], John Smellie (ed.)[2]
[1] AECL, Canada
[2] Conterra AB, Uppsala, Sweden
May 1994

TR 94-05
Tectonic regimes in the Baltic Shield during the last 1200 Ma - A review
Sven Åke Larsson[1,2], Eva-Lena Tullborg[2]
[1] Department of Geology, Chalmers University of Technology/Göteborg University
[2] Terralogica AB
November 1993

TR 94-06
First workshop on design and construction of deep repositories - Theme: Excavation through water-conducting major fracture zones Såstaholm Sweden, March 30-31 1993
Göran Bäckblom (ed.), Christer Svemar (ed.)
Swedish Nuclear Fuel & Waste Management Co, SKB
January 1994

TR 94-07
INTRAVAL Working Group 2 summary report on Phase 2 analysis of the Finnsjön test case
Peter Andersson (ed.)[1], Anders Winberg (ed.)[2]
[1] GEOSIGMA, Uppsala, Sweden
[2] Conterra, Göteborg, Sweden
January 1994

TR 94-08
The structure of conceptual models with application to the Äspö HRL Project
Olle Olsson[1], Göran Bäckblom[2], Gunnar Gustafson[3], Ingvar Rhén[4], Roy Stanfors[5], Peter Wikberg[2]
1 Conterra AB
2 SKB
3 CTH
4 VBB/VIAK
5 RS Consulting
May 1994

TR 94-09
Tectonic framework of the Hanö Bay area, southern Baltic Sea
Kjell O Wannäs, Tom Flodén
Institutionen för geologi och geokemi, Stockholms universitet
June 1994

TR 94-10
Project Caesium--An ion exchange model for the prediction of distribution coefficients of caesium in bentonite
Hans Wanner[1], Yngve Albinsson[2], Erich Wieland[1]
[1] MBT Umwelttechnik AG, Zürich, Switzerland
[2] Chalmers University of Technology, Gothenburg, Sweden
June 1994

TR 94-11
Äspö Hard Rock Laboratory Annual Report 1993
SKB
June 1994

TR 94-12
Research on corrosion aspects of the Advanced Cold Process Canister
D J Blackwood, A R Hoch, C C Naish, A Rance, S M Sharland
AEA Technology, Harwell Laboratory, UK
January 1994

TR 94-13
Assessment study of the stresses induced by corrosion in the Advanced Cold Process Canister
A R Hoch, S M Sharland
Chemical Studies Department, Radwaste Disposal Division, AEA Decommissioning and Radwaste, Harwell Laboratory, UK
October 1993

TR 94-14
Performance of the SKB Copper/Steel Canister
Hans Widén[1], Patrik Sellin[2]
[1] Kemakta Konsult AB, Stockholm, Sweden
[2] Svensk Kärnbränslehantering AB, Stockholm, Sweden
September 1994

TR 94-15
Modelling of nitric acid production in the Advanced Cold Process Canister due to irradiation of moist air
J Henshaw
AEA Technology, Decommissioning & Waste Management/Reactor Services, Harwell, UK
January 1994

TR 94-16
Kinetic and thermodynamic studies of uranium minerals. Assessment of the long-term evolution of spent nuclear fuel
Ignasi Casas[1], Jordi Bruno[1], Esther Cera[1], Robert J Finch[2], Rodney C Ewing[2]
[1] MBT Tecnología Ambiental, Cerdanyola, Spain
[2] Department of Earth and Planetary Sciences, University of New Mexico, Albuquerque, NM, USA
October 1994

TR 94-17
Summary report of the experiences from TVO's site investigations
Antti Öhberg[1], Pauli Saksa[2], Henry Ahokas[2], Paula Ruotsalainen[2], Margit Snellman[3]
[1] Saanio & Riekkola Consulting Engineers, Helsinki, Finland
[2] Fintact Ky, Helsinki, Finland
[3] Imatran Voima Oy, Helsinki, Finland
May 1994

TR 94-18
AECL strategy for surface-based investigations of potential disposal sites and the development of a geosphere model for a site
S H Whitaker, A Brown, C C Davison, M Gascoyne, G S Lodha, D R Stevenson, G A Thorne, D Tomsons
AECL Research, Whiteshell Laboratories, Pinawa, Manitoba, Canada
May 1994

TR 94-19
Deep drilling KLX 02. Drilling and documentation of a 1700 m deep borehole at Laxemar, Sweden
O Andersson
VBB VIAK AB, Malmö
August 1994

TR 94-20
Technology and costs for decommissioning the Swedish nuclear power plants
Swedish Nuclear Fuel and Waste Management Co, Stockholm, Sweden
June 1994

TR 94-21
Verification of HYDRASTAR: Analysis of hydraulic conductivity fields and dispersion
S T Morris, K A Cliffe
AEA Technology, Harwell, UK
October 1994

TR 94-22
Evaluation of stationary and non-stationary geostatistical models for inferring hydraulic conductivity values at Äspö
Paul R La Pointe
Golder Associates Inc., Seattle, WA, USA
November 1994

TR 94-23
PLAN 94
Costs for management of the radioactive waste from nuclear power production
Swedish Nuclear Fuel and Waste Management Co
June 1994

TR 94-24
Äspö Hard Rock Laboratory
Feasibility and usefulness of site investigation methods. Experiences from the pre-investigation phase
Karl-Erik Almén (ed.)[1], Pär Olsson[2], Ingvar Rhén[3], Roy Stanfors[4], Peter Wikberg[5]
[1] KEA GEO-Konsult
[2] SKANSKA
[3] VBB/VIAK
[4] RS Consulting
[5] SKB
August 1994

TR 94-25
Kinetic modelling of bentonite-canister interaction. Long-term predictions of copper canister corrosion under oxic and anoxic conditions
Paul Wersin, Kastriot Spahiu, Jordi Bruno
MBT Tecnología Ambiental, Cerdanyola, Spain
September 1994

TR 94-26
A surface chemical model of the bentonite-water interface and its implications for modelling the near field chemistry in a repository for spent fuel
Erich Wieland[1], Hans Wanner[1], Yngve Albinsson[2], Paul Wersin[3], Ola Karnland[4]
[1] MBT Umwelttechnik AG, Zürich, Switzerland
[2] Chalmers University of Technology, Gothenburg, Sweden
[3] MBT Tecnología Ambiental, Cerdanyola, Spain
[4] Clay Technology AB, Lund, Sweden
July 1994

TR 94-27
Experimental study of strontium sorption on fissure filling material
Trygve E Eriksen, Daqing Cui
Department of Chemistry, Nuclear Chemistry, Royal Institute of Technology, Stockholm, Sweden
December 1994

TR 94-28
Scenario development methodologies
Torsten Eng[1], John Hudson[2], Ove Stephansson[3], Kristina Skagius[4], Marie Wiborgh[4]
[1] Swedish Nuclear Fuel & Waste Management Co, Stockholm, Sweden
[2] Rock Engineering Consultants, Welwyn Garden City, Herts, UK
[3] Div. of Engineering Geology, Royal Institute of Technology, Stockholm, Sweden
[4] Kemakta, Stockholm, Sweden
November 1994

TR 94-29
Heat conductivity of buffer materials
Lennart Börgesson, Anders Fredrikson, Lars-Erik Johannesson
Clay Technology AB, Lund, Sweden
November 1994

TR 94-30
Calibration with respect to hydraulic head measurements in stochastic simulation of groundwater flow – A numeric experiment using MATLAB
L.O. Eriksson, J Oppelstrup
Starprog AB
December 1994